Characterization of Phytoplankton Community Changes in Barnegat Bay Related to the Closure of Oyster Creek Nuclear Generating Station, Combining Next Generation Sequencing and Microscopic Analyses

Final Report

Project funded by New Jersey Department of Environmental Protection (NJDEP)
through an Agreement with New Jersey Sea Grant Consortium (NJSGC)

NJDEP No. SR20-008
NJSGC No. 4904-0045

Prepared for

Division of Science and Research

New Jersey Department of Environmental Protection

Prepared by

Ling Ren, Ph.D.

Department of Environmental Science and Policy (ESP)
College of Science, George Mason University
4400 University Dr. Fairfax, VA 22030

and

Patrick M. Gillevet, Ph.D. & Masoumeh Sikaroodi, Ph.D.

MicroBiome Analysis Center (MBAC), Department of Biology
College of Science, George Mason University
4400 University Dr. Fairfax, VA 22030

May 2024

Acknowledgements

We sincerely thank Robert Schuster, Eric Ernst, Dawn Thompson, and the field and lab crew of the NJDEP's Bureau of Marine Water Monitoring for their help and for water sample collections and filtration for DNA sequencing. We are thankful to Drs. Mihaela Enache and Joseph Bilinski of the NJDEP's Division of Science and Research for their management and support with this project. Our sincere thanks to Drs. Metthea Yepsen and Nick Procopio for their reviews and constructive comments to improve the reports. This work is funded by NJDEP through the NJ Sea Grant Consortium (NJDEP No. SR20-008, NJSGC No. 4904-0045).

Recommended Citation:

Ren, L., Gillevet, P. M., Sikaroodi, M., Enache, M., 2024. Characterization of Phytoplankton Community Changes in Barnegat Bay Related to the Closure of Oyster Creek Nuclear Generating Station, Combining Next Generation Sequencing and Microscopic Analyses (Final Report). New Jersey Department of Environmental Protection. Trenton, NJ. 72 pages. Available at DSPACE web link: https://hdl.handle.net/10929/137567

Table of Contents

Project Summary

Following Exelon Inc.'s announcement that the Oyster Creek Nuclear Generating Station (OCNGS) would cease operation ahead of planned decommissioning in 2029, the NJDEP engaged with researchers to begin an investigation to determine what impacts to marine biota (i.e., phytoplankton, zooplankton, benthic invertebrates, fish, and crabs) may occur because of the plant shutdown. Our project was designed specifically to examine the influence on phytoplankton community composition and dynamics. This report comprises a comprehensive analysis comparing all three years of OCNGS post-closure (2018-2021) phytoplankton data to baseline data collected between 2012-2017 as part of the Barnegat Bay Comprehensive Research Initiative, thus in effect the "final report" for this study (see NJDEP| Division of Science and Research | Barnegat Bay). This report also contains the analysis and interpretation of data generated in Year 3 (2020-2021) of the OCNGS project effort. Additional information on the findings of the preceding studies can be found at: NJDEP| Division of Science and Research | Oyster Creek Nuclear Generating Station.

Impact of OCNGS Closure

To understand the impact of OCNGS decommissioning, phytoplankton from the three-year (2018-2021) study were compared with the baseline study from 2012-2017, performed under the Barnegat Bay Comprehensive Research Initiative. Water quality data, retrieved from EPA's Water Quality Portal, was compiled from 2014 to 2021. Multivariate analyses were performed to examine the variability of water quality data for this period, explore correlations between environmental variables, and their relationships with phytoplankton community changes. Results from these analyses were used to assess the changes that occurred 'before' and 'after' the OCNGS closure. The before-closure dataset contains the monthly/biweekly measurements from April 2014 to August 2018, and the after-closure dataset includes the measurements from September 2018 to December 2021.

Both microscopy and DNA-based data collected between 2018-2021 showed high dynamics of temporal and spatial variations of phytoplankton at the 6 sites (BB01, BB05a, BB07a, BB09, 1661A, 1663A) sampled in Barnegat Bay. Phytoplankton community composition at the same site showed prominent seasonality every year. The inter-annual variability of phytoplankton, over the three years, was generally overlapped by seasonality which is driven by temperature. High year-to-year variability was exhibited when comparing phytoplankton from the same month. The characteristics of temporal variations varied between the sites. High dynamics of phytoplankton changes from this study period are consistent with the data collected from 2014-2017 in Barnegat Bay for sites BB01, BB07a, and BB09.

The impact of the OCNGS shutdown was assessed by comparing the environmental variables and phytoplankton at 1661A, 1663A, and BB07a before and after the beginning of decommissioning in the week of September 17, 2018. 1661A is located at the mouth of Forked River, and 1663A at the mouth of Oyster Creek. BB07a is located southeast of 1663A, a Barnegat Bay site close to the OCNGS. In addition, BB01, located at the northern end of Barnegat Bay, and BB09, close to Barnegat Inlet, were used as reference sites as both sites are further from the OCNGS.

Water quality data showed salinity drops of 4-8 ppts at sites BB07a, 1661A and 1663A in response to the steps of the shutdown in 2018, suggesting an increased influence of freshwater in the area. In the following fall-winter of 2019-2021, a slight increase followed by high variability of salinity was detected at these three sites. Monthly data showed that temperature at 1663A was generally higher than 1661A (Forked River intake point for reactor cooling water) before the decommission owing to the discharge of cooling water from OCNGS near 1663A. After the first step of shutdown, the temperature between these two sites became very similar. The temperature drops and water circulation alteration did not seem abrupt and significant as in previous cases, indicating the effectiveness of a stepwise decommission strategy. Although these findings did not reveal a permanent decrease in salinity near the mouths of Forked River and Oyster Creek, a shift in salinity and nutrients relationships was recorded for the post-OCNGS closure period, suggesting an increased effect of freshwater input in the salinity-nutrients dynamics in this area of Barnegat Bay, as described below.

Principal component analysis (PCA) revealed a positive relationship between salinity and nutrients before the shutdown at BB07a, BB01 and BB09. After the shutdown, nutrients were in reverse relationship to salinity at BB07a and BB09, whereas at BB01which is furthest from the OCNGS, salinity and nutrients showed no or weak relation. The shutdown of OCNGS has resulted in more direct freshwater inflows from Oyster Creek, which in turn enriched nutrients in the area near BB07a, and possibly BB09 as well.

Canonical Correspondence Analysis (CCA) showed the changes of phytoplankton communities were significantly affected by environmental variables. The environmental variables explained about 38% to over 53% of phytoplankton changes at BB01, BB07a, and BB09. There was an increase of the explanatory power of the environmental variables for all the three sites after the OCNGS closure, but with BB07a increasing the most and BB01 the least, coincident with their distances from the OCNGS. As the effects of the environmental variables and man-made

activities can often be intertwined, such difference could be an indication of reduced impact from OCNGS after the decommission.

The differences of phytoplankton between the mouth of Forked River (site 1661A) and that of Oyster Creek (site 1663A) were greater in August 2018 compared to October 2018, coincident with the first step in the shutdown of OCNGS. Furthermore, the subsequent dissimilarity in November samples between these 2 sites and more similarity in December samples coincided with the shutdown of the secondary circulation pumps in November 2018. In 2019 and 2021, the communities at these two sites became more similar for most months, except for March, April, August, and December 2021 when the differences are comparable to that in August 2018, possibly owing to the localized and short-term hydrological, chemical, and biological factors.

Comparison of the phytoplankton at BB07a was done between the August samples from 2012 to 2021 when the effects of temperature were minimized. The variability of the August samples between 2018 vs. 2019 was comparable to that between 2012 vs. 2013, when the latter was heavily impacted by Hurricane Sandy. Of the September samples from 2014 to 2021, the largest dissimilarity was detected from 2018 vs. 2019, while the October samples also showed higher distance from 2018 vs. 2019 of years from 2014-2021. However, during the multiple years, from observing the variations in phytoplankton data, there is a lot of variation that is higher in many instances than the differences between sampling events made in August to October can be found in the other years and stations.

It is worth noting that the water quality and phytoplankton data were collected monthly. The change of temperature and water circulation following the shutdown happened in a relatively shorter time and may not be captured through monthly samplings. The changes observed at the study sites as a result of the OCNGS decommission are difficult to disentangle from the regular and very dynamic hydrological, chemical, and biological processes taking place in Barnegat Bay. In addition, the impact of weather conditions, such as wind and precipitations, and tides and small-scale water advection and circulations are not considered throughout the sampling periods.

Phytoplankton Metabarcoding

We compared 16S rRNA barcoding with the microscopy method on phytoplankton classifications, and tested three sets of 18S rDNA primer sets to improve the classification resolutions of eukaryotic phytoplankton.

Results from the present study proved that metabarcoding can serve well as a complementary tool to the microscopic analysis in phytoplankton biomonitoring, and in some cases, can be a better approach. The combination of the 16S rRNA marker and Next-generation sequencing

generated high-throughput data and provided information on photosynthetic cyanobacteria and eukaryotic phytoplankton, community diversity and composition, as well as relative abundance of major taxonomic groups. Although limitation exists in the classification resolution for nano-phytoplankton, the method was superior to light microscopy in the case of picoplankton and was able to distinguish major groups in the picoplankton complex which are often challenging by traditional microscopy methods. In addition, our study based on the 18S rDNA primer sets identified some existing gaps in sequence databases and provides a foundation for further research in developing metabarcoding.

Introduction

Project Background

Oyster Creek Nuclear Generating Station (OCNGS) is the oldest operating commercial nuclear power plant in the United States and began operating in December 1969. The facility is located between the South Branch of Forked River and Oyster Creek in Ocean County, about 3.2 km inland from Barnegat Bay, New Jersey (Fig. 1). The facility consists of a single unit of boiling water reactor with a once-through cooling water system. The system intakes water from Forked River through two surface water intake structures: the Circulating Water Intake, which withdraws water up to an amount of 662 million gallons per day (MGD) to cool the reactor, and the Dilution Water Intake, which withdraws up to 732 MGD of water to moderate the thermal effects from the cooling water. All intake water is discharged into Oyster Creek via a discharge canal and further downstream to Barnegat Bay.

During normal operations, impingement, entrainment, and thermal effects are the major concerns to fishery resources and natural populations in the area. Large organisms, mainly fish and crabs, can be trapped on the intake screens and trash racks and become impinged. Small organisms which are entrained to the cooling system will be exposed to a sudden temperature rise of 12-13 °C and up and a lethal level of chlorine (Summers et al. 1989). Surviving organisms continue to be exposed the excessive temperature while transiting down the discharge canal. In addition, organisms in receiving waters can be exposed to elevated temperatures in the discharge plume. During operation the facility also releases about 3.53 MGD wastewater and approximately 3.5 MGD chlorinated washwater from the radioactive waste treatment. Chlorine is considered toxic to most of the estuarine biota at the range of ppb to ppm and its toxicity is at greatest at high temperature. In addition, the discharge water may include residues of copper corroded from the condenser tubes, small amount of sodium, phosphorus, sulfates, chlorides, iron, oil and grease, and low levels of radioactivity, though, prior to discharge, wastewater discharges were analyzed to make sure the amount of radioactivity is within the acceptable limits (Summers et al. 1989).

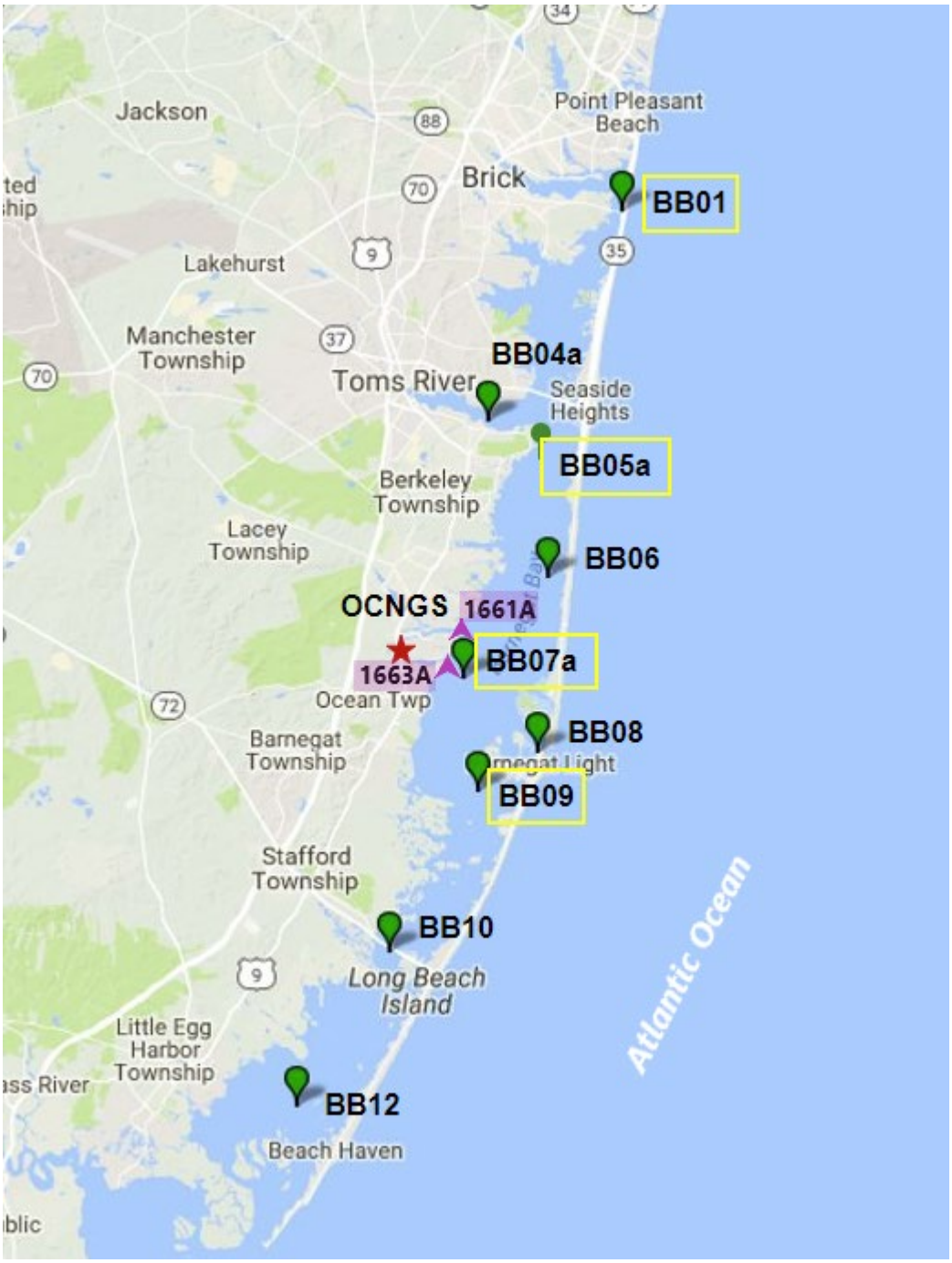

Fig. 1. Location of sampling sites for this project. Sites with yellow border were sampled starting in 2012 when the Barnegat Bay phytoplankton baseline study began. Pink highlighted sites 1661A and 1663A are located closest to OCNGS (star symbol) and together with site BB07a represent OCNGS impacted sites. BB01 and BB09 represent reference sites in the 2018-2021 study.

Decommission of the OCNGS

Decommission of the OCNGS has gone through multiple steps to ease the impact on surrounding ecosystems from an abrupt shutdown. First, the two largest dilution pumps, out of 4, were shut down during the week of September 17th, 2018, which resulted in a total reduced flow of 1 million gallons per minute (1/2 million gallons per minute each pump); Second, most of circulation pumps were shut down at the beginning of November 2018, which left the plant operating only 1 circulation pump and 2 service pumps, each with a flow rate of approximately 6,000 gallons per minute; Third, the OCNGS was drawing 12,000 – 24,000 Gallons per minute of water by the end of 2018; Fourth: one more service pump was shut down in the first quarter of 2019. Prior to the decommission, the OCNGS system withdrew water from the Forked River and discharged it into Oyster Creek via a discharge canal and further downstream to Barnegat Bay. Following these shutdown steps, the withdrawal and discharge rates have been reduced by more than 95%.

The anticipated physical changes related to the closure of the OCNGS included the immediate and sharp temperature drops in Oyster Creek and milder temperature decrease in Barnegat Bay as a secondary receiving water body. The operation of OCNGS showed a 1.5°F above ambient summer thermal plume extending completely across Barnegat Bay. Such thermal effect would be almost removed after the OCNGS closure. Meanwhile, the largely reduced discharge can lead to the alteration of the water circulation patterns in mid-Barnegat Bay. It is important for us to understand and evaluate how the closure of OCNGS affected the development of fishery resources and other biota populations, as well as the ecology and water quality in the adjacent Barnegat Bay.

Phytoplankton Metabarcoding

Phytoplankton are comprised of a diverse and polyphyletic group that encompasses organisms from widely different taxonomic domains, including eukaryotes and prokaryotes. Metabarcoding proved to be a robust and reliable method for qualitative and semiquantitative analysis in plankton research (Abad et al. 2016, Bush et al. 2019). This method allows us to analyze large amounts of samples with the same sensitivity and with time and cost effectiveness, although potential bias and limitations are recognized in many steps of metabarcoding development (Ruppert et al. 2019, Santoferrara 2019). Two key components in phytoplankton metabarcoding are 1) adequate PCR primers that can simultaneously prioritize the sequencing of highly informative regions (Hugerth et al. 2014); 2) comprehensive DNA barcode reference libraries that can provide reliable biodiversity and taxonomic information for wide ranges of aquatic samples (Weigand et al. 2019). We attempted to develop phytoplankton metabarcoding using 16S rRNA markers and Next-Generation (NextGen) Sequencing for the taxonomic classification

of cyanobacteria and autotrophic phytoplankton based on chloroplast sequences, and to test using 18S rDNA primers for the classifications of eukaryotic phytoplankton.

Project Objectives

The overall objective of the project was to characterize the changes in phytoplankton community before and after the closure of OCNGS, and to evaluate the impact of the OCNGS shutdown on the biological and ecological structures of Barnegat Bay and its tributaries adjacent to OCNGS. We aimed to assess the short-term (months) and long-term (years) changes of phytoplankton by comparing the post-closure phytoplankton data with the pre-closure data collected between 2012 and August 2018 from 3 stations across Barnegat Bay. In addition, we attempted to test and develop the application of metabarcoding for routine monitoring of coastal phytoplankton by comparing traditional microscopy observations with the results from the NextGen DNA Sequencing technique.

Under the Barnegat Bay Phase II program (NJDEP-Barnegat Bay), three years of study were carried out between 2018 and 2021 with the interruption of the Pandemic in 2020. During the study period, phytoplankton composition was monitored at six sites in Barnegat Bay to characterize the temporal and spatial changes of phytoplankton with a focus on those closer to the OCNGS and near the Forked River and Oyster Creek. Monthly samples were collected in 2018, 2019, 2020 and 2021, for analysis of phytoplankton using microscopy,DNA sequencing and barcoding methods.

Materials and Methods

Sample Collection

Water samples were collected from April to December 2018 at four sites in the northern and central segments of Barnegat Bay, BB01, BB05a, BB07a and BB09. Special focus was on BB07a, the site closest to OCNGS, and BB09 and BB01 at the farther locations, were used as reference sites. In addition, samples from the sites in the mouths of the Forked River (1661A) and Oyster Creek (1663A) were collected from August 2018 to provide information from the sites that are located closer to the OCNGS than the regular sites in the previous Barnegat Bay studies. Additional samples collected from sites BB01, BB07a and BB09 from October to December 2017 were analyzed as pre-closure data. The location and description of the sites are shown in Fig. 1 and Table 1. In the following years, monthly samples were continuously collected from January to December 2019, January to March 2020, and January to December 2021 from the same six sites (BB01, BB05a, BB07a, BB09, 1661A and 1663A). In total, 197 samples were analyzed with traditional microcopy and 215 samples were done using DNA sequencing method for phytoplankton classification and composition.

Sample collections were coordinated with the NJDEP's Barnegat Bay Water Quality Monitoring Program and carried out by the DEP's Bureau of Marine Water Monitoring (BMWM). All water samples were collected at a depth of ~0.5 feet below the surface at each site. For each sample, two types of subsamples were processed, one for microscopic counting and one for DNA sequencing, respectively. Water samples for microscopy were preserved with glutaraldehyde (0.5% ~1% v/v) and kept dark and cool (~ 4 °C) prior to analysis. Subsamples for DNA sequencing, about 50-100 ml sample water, were filtered through 0.2-µm pore-size polycarbonate membranes. The membranes were kept frozen prior to laboratory analysis.

Table 1. Description of study sites for phytoplankton in Barnegat Bay from 2018 to 2021.

Site ID	Longitude	Latitude	Site description
BB01	-74.052222	40.04	Barnegat Bay at Mantoloking
BB05a	-74.1094237	39.9157764	Barnegat Bay above Cedar Creek
BB07a	-74.1571172	39.8012861	Barnegat Bay below Oyster Creek and above Barnegat Inlet
BB09	-74.14792	39.74262	Barnegat Bay below Barnegat Inlet and close to Long Beach
1661A	-74.1577778	39.8250083	near the mouth of Forked River
1663A	-74. 1655556	39. 8090889	Near the mouth of Oyster Creek

Microscopic Analysis

Phytoplankton analysis through light microscopy identification and counting followed the same methods throughout the 3-year study, as described below.

Water samples were size-fractionated by filtering through 0.2 µm, 3 µm and 8 µm pore-size filter membranes. The latter two fractions were stained with 0.03% proflavine hemisulfate. The 0.2 to 3 µm fraction was counted immediately after filtration. The >8 µm fraction was kept frozen and counted later but no later than one week. Phytoplankton identification and enumeration were done under an epifluorescence microscope (Leica DM L 2) with blue and green excitation lights and transmitted light. For 0.2 and 3 µm pore-size filters, observations were done under ×1000 magnification. For each filter, at least 5 random fields were counted or until at least 100 cells were reached. If phytoplankton on the filter were very sparse, 50 random fields were counted before stopping. For 8 µm pore-size filters, each filter was observed under three magnifications: under ×1000 magnification for phytoplankton <20 µm with the same counting strategy in terms of finishing point; under ×400 magnification for larger (>20 µm) phytoplankton with a maximum of 25 random fields when it was sparse; and under ×100 magnification to catch any large organisms which might have been missed under higher magnifications due to either their large size or low density. The detection limit is approximately 500 to 1000 cells/L, depending on

the sample volume filtered (Dortch et al. 1997; Ren et al. 2009). All phytoplankton were identified to the lowest taxonomic level possible.

DNA Work

Several steps were taken in the laboratory analyses to analyze the filter samples for phytoplankton classification and composition, including DNA extraction and purification, polymerase chain reaction (PCR) amplification, LH-PCR fingerprinting, and multitag Next-Generation Sequencing. In addition, bioinformatic analyses were carried out using RDP 11 (Ribosomal Database Project) and BLASTn (Basic Local Alignment Search Tool). A schematic diagram of the molecular analyses on phytoplankton samples is illustrated (Fig. 2).

DNA extraction and purification

Total genomic DNA was extracted from filter samples using "BIO101-FastDNA Spin Kit for Soil" made by MP Biomedicals Inc., Montreal, Quebec as per the manufacturer's instructions. A dilution of the DNA was made (usually 1:5 dilution with 0.1X TE buffer) to avoid freeze-thawing the samples and the original DNA is kept at -80^{o}C freezer for long-term storage.

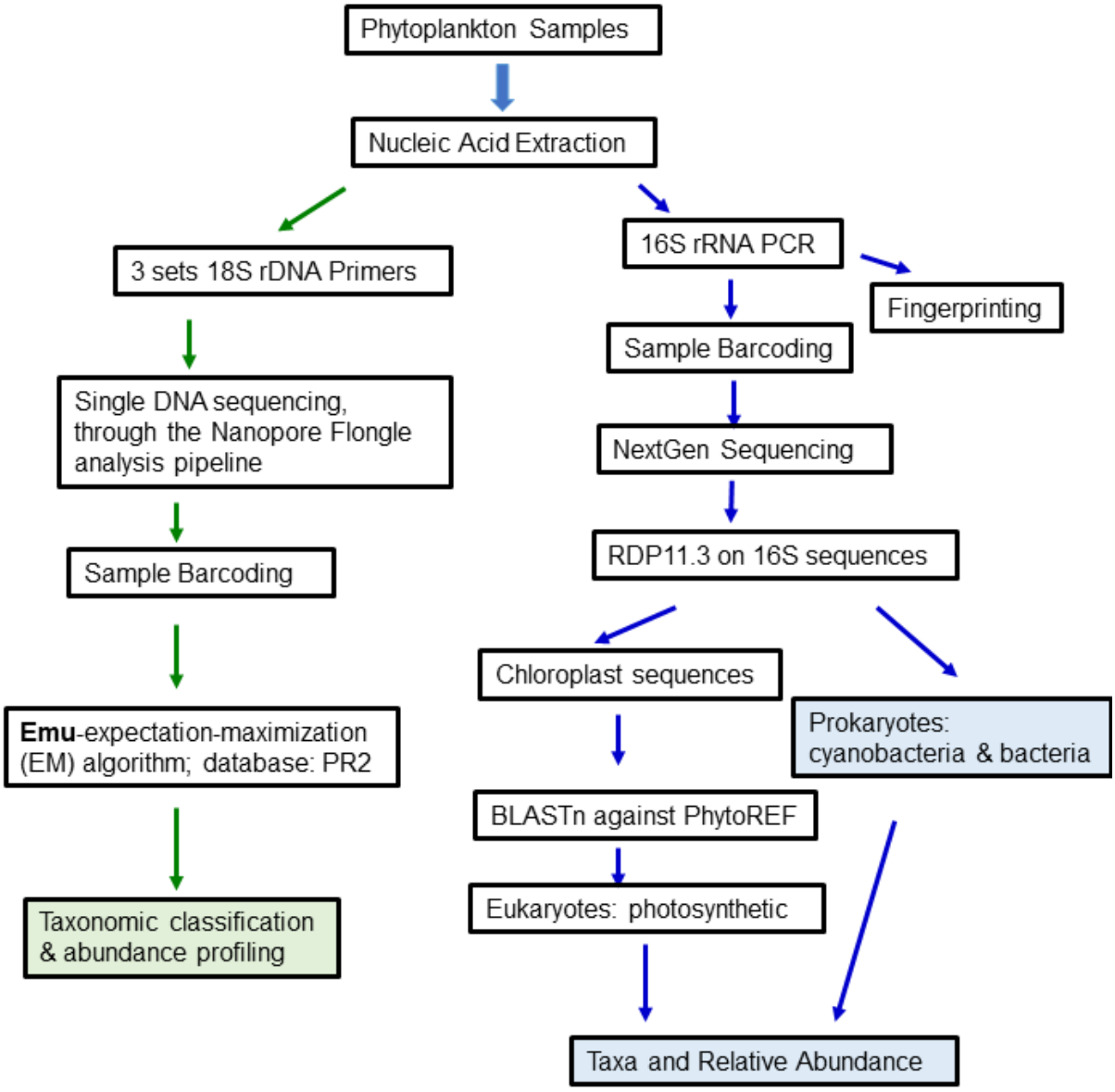

Fig. 2. Schematic diagram of the molecular work on phytoplankton metabarcoding.

PCR amplification and LH-PCR fingerprinting

DNA fragments were then amplified by polymerase chain reaction (PCR) with a universal16S rRNA primer or 18S DNA primer sets, as the first step. Duplicate PCR was done to test the dilution and optimize the conditions for different samples. Some samples may have to be diluted further (to 1:10 or 1:100) or for some we may have to use the original DNA. The PCR products were visualized with ethidium bromide and diluted with diH2O from 1:10 to 1:30 of ratios based on their intensity, and then added to ILS-600 (internal lane standard from Promega) and HiDi formamide (Applied Biosystems) mix in 1:10 ratio (1 part diluted PCR product and 9 parts ILS mix). ILS-600 and HiDi Formamide mixture was made in a 1:20 ratio (one-part ILS600 and 19 parts HiDi Formamide). The mixture was run on a capillary electrophoresis instrument (ABI3130XL) for fingerprinting and comparing the complexity of the community by determining the size of the OTU (Operational Taxonomic Unit) peaks. Duplicates or triplicates were done on each DNA sample to compare the replicability and consistency of the PCR results. The fingerprinting was done as quality control to determine the reproducibility and reliability in PCR. The fingerprint results were analyzed and visualized using Genemapper v4.1 software (http://tools.thermofisher.com/content/sfs/manuals/cms_070157.pdf).

Multitag Next-Generation (NextGen) Sequencing

The DNA samples that worked best in PCR were pooled for NextGen Sequencing. The second PCR was performed for each sample under the same conditions as the first PCR. Multitag technique was used to sequence samples, which allows the rapid sequencing of multiple samples at one time, yielding thousands of sequence reads per sample.

16S rRNA sequencing

We used a universal 16S rRNA primer, 27F forward (5'AGAGTTTGATCMTGGCTCAG3') and 355R reverse (5'ACTCCTACGGGAGGCAGC3'), to detect cyanobacteria and eukaryotic phytoplankton based on the chloroplast sequences. The step generated a set of 96 emulsion PCR fusion primers that contain the Ion Torrent emulsion PCR linkers and different 8 base "barcode" on either of the 27F or 355R of universal 16S rRNA primers (Gillevet et al. 2010). Each sample was amplified with a uniquely barcoded set of forward and reverse 16S rRNA primers. Both primers have specific adaptors to use with Ion Torrent technology and the forward primers have a barcode (or tag) incorporated into the primer sequence to be able to differentiate the sequences in different samples. Up to 48 samples were pooled and the sample pool was purified using Ampure solution (Beckman Coulter) to remove any primers or extra nucleotides. After quantitating the purified products, the NGS sequencing was performed using Ion Torrent technology (Life Techonologies) following the manufacturer's protocols (http://tools.thermofisher.com/content/sfs/manuals/MAN0007273_IonPGMSequenc_200Kit_v2_UG.pdf). Data from each pooled sample was "deconvoluted" by sorting the sequences into bins

based on the barcodes using custom PERL scripts, to normalize each sample by the total number of reads from each barcode. The data was initially analyzed with Ion Torrent software which produces a *fastq* file. A Pearl script was written to de-multiplex the sequences and to assign the right IDs to samples based on the barcodes (or tags). The resulting *fasta* file was uploaded into Galaxy portal on the Microbiome Analysis Center (MBAC) website (http://mbac.gmu.edu) for further analyses.

18S rDNA sequencing

Three (3) sets of the 18S rDNA primer pairs were selected through a thorough literature because of their effectiveness and coverage of eukaryotic microalgae (Zimmermann et al. 2011, Esenkulova et al. 2020, Vaulot et al. 2022), and further checked against Silva Test Prime (https://www.arb-silva.de/search/testprime) and BLASTn analysis against NCBI (Table 2 and references therein). Twenty-four (24) samples, from January, March, May and August 2021 and representative of species diversity and variations based on the microscopic observations, were selected for the test runs of the three sets of 18S primers. DNA samples were sequenced using Oxford Nanopore technology through the Nanopore Flongle analysis pipeline which sequences single DNA molecules as it passes through a pore in an artificial charge clamped membrane. This technology was originally applied in the16S rRNA sequencing and showed high accuracy (99%) in microbiome classifications at the species level (Kerkhof et al. 2017). We applied state-of-art technology to sequence the key informative regions of the 18S rRNA gene, using three primer pairs (Oxy18S, euk18S, and D18S) to obtain the most taxonomic information to classify the phytoplankton to the species level. The Oxford Nanopore Rapid Sequencing Kit SQK_RPB114.24 and Flongle Expansion kit EXP_FSE001 were used to run the amplified products on the Flongle. This work was done on a PC with a NVIDIA GPU board (RTX A400) which has 6,144 CUDA cores to allow base calling in real time.

Bioinformatic analyses on 16S rRNA sequences

Bioinformatic analyses on 16S rRNA sequences were carried out using RDP 11.3 (Ribosomal Database Project) and BLASTn (Basic Local Alignment Search Tool) for taxonomic classification and relative abundance of each sample.

RDP 11.3 analysis

Ribosomal Database Project (RDP) 11.3 (http://rdp.cme.msu.edu/) was applied to analyze rRNA gene sequences for taxonomic classification and relative abundance of each taxon (Cole et al. 2013). The relative abundance of the taxa was calculated using a custom PERL script and taxa present at > 0.1% of the community was tabulated. The OTUs constituting less than 0.1% of the total community from each sample were eliminated from the analysis, with *a priori* assumption that the low abundance components of the community vary between individual subjects and do

not contribute significantly to the functionality of the whole community. In RDP 11.3 analysis, the classification with the correlation bootstrap greater than 0.60 is considered a 'true' identity, the classification with bootstrap between 0.60 and 0.10 is noted with 'other' and those with bootstrap less than 0.10 are classified as 'unknown'. The standard nucleotide BLASTn analysis was performed on 16S rRNA sequences against the GenBank 16S Microbial Database at National Center for Biotechnology Information (NCBI) (https://blast.ncbi.nlm.nih.gov/). The database Nucleotide Collection (nr/nt) with the exclusion of uncultured/environmental sequences was selected for taxonomic classification (Zhang et al. 2000). Prokaryotic communities, including bacteria and cyanobacteria, were identified at the taxonomic levels of genus, species, and strains. The taxa, which made up a relative abundance >0.1% of the whole community, was presented and analyzed in the results.

BLASTn analysis against PhytoREF

We tested the applicability of using the 16S rRNA gene as a taxonomic marker for the classification of autotropic organisms (Yoon et al. 2016, Bennke et al. 2018). The BLASTn analysis was carried out against an online database PhytoREF (http://phytoref.sb-roscoff.fr/; accessed January 2024). The database contains 6490 plastidial 16S rDNA reference sequences from a large diversity of eukaryotes representing all known major photosynthetic lineages. It includes 6490 plastidial 16S rDNA reference sequences originating from a large diversity of eukaryotes representing all known major photosynthetic lineages. The database also contained 554 cyanobacteria classifications, and most of the classifications are to the family or genus level (Decelle et al. 2015).

Bioinformatic analyses on 18S rDNA sequences

The 18S full length reads were then trimmed using the Barcode trimmer in the MinKnow software package and converted to MBAC format that tracks the Sample-ID with each Read-ID using a custom PERL script. Data is then transferred to a 48 core, 3TB memory HP server.

The reads were then processed using Emu, which is a microbial community profiling software tool tailored for full-length ribosomal RNA data (Curry et al. 2022). Emu's algorithm involved a two-stage process. First, proper alignments were generated between reads and the supplied reference database using minimap2. The PR2 database (Guillou 2013, Vaulot et al. 2022), used as a reference database for this study, was formatted to be compatible with the Emu data structure (Curry et al. 2022) using a custom PERL script. Then, as the second stage, the Expectation-Maximization (EM) based error-correction is performed to iteratively refine species-level relative abundances based on total read-mapping counts. This method provides microbial community profile estimations from full-length DNA sequence reads, which are more accurate than existing methods at both the genus and species level. We then used a custom PERL script to

parse the two Emu output files to construct sample abundance tables for each of the taxonomic levels down to the species level.

Table 2: Three sets of 18S rDNA primers tested on 2021 samples for eukaryotic phytoplankton classifications.

Primer Sets	Primer direction	Sequences (5'-3')	Reference
V3 87 Oxy	Forward: Oxy 18S F	ATCAGAWACCGYCGTAGTC	Vaulot et al. 2021
	Reverse: Oxy 18S-R	GGGCATMACRGACCTGTTA	
18S-Dino	Forward: euk-A7F	AACCTGGTTGATCCTGCCAGT	Esenkulova_etal. 2020
	Reverse: euk-570R	GCTATTGGAGCTGGAATTAC	
PhytoD	Forward: D512for 18S	ATT CCA GCT CCA ATA GCG	Zimmermann et al. 2011; Esenkulova_etal. 2020
	Reverse: D978rev 18S	GAC TAC GAT GGT ATC TAA TC	

Water quality data

Monthly water quality data were downloaded from EPA's Water Quality Portal (https://www.epa.gov/waterdata/water-quality-data-download, accessed May 2022) for the 6 sites in Barnegat Bay from 2018 to 2021. In addition, water quality data for the sites BB01, BB07a and BB09 were retrieved from 2012 to 2017 for the comparison of before and after the decommission of OCNGS.

Statistical Analyses

Principal Coordinates analysis (PCO, or PCoA)**,** also known as metric multidimensional scaling, was used to compare phytoplankton communities among different sites and different time periods. The Bray-Curtis method was used to calculate the sample distances for the PCO analysis. This method is an ordination technique, calculating the similarity (dissimilarity) in species composition among each pair of samples in consideration of their quantitative values. The PCO method was applied to investigate the differences in community among sites and seasons from both microscopic and DNA sequencing analyses. PCO is similar to nonmetric multidimensional scaling method (NMDS) in terms of analyzing community data, however, NMDS considers only the rank order of the dissimilarity (similarity), whereas PCO considers their quantitative values.

Principal Components Analysis (PCA) is an ordination method that enables us to simplify the complexity in high-dimensional data while retaining trends and patterns. PCA analysis was performed to investigate correlations between the environmental variables.

Canonical Correspondence Analysis (CCA) was conducted to elucidate the relationships between community changes and environmental variables. CCA is a multivariate constrained ordination technique that calculates a weighted reciprocal average of the species data and performs a multiple least squares regression of the species data onto explanatory variables.

The analyses of PCO, PCA and CCA were carried out using the program Canoco 5.0 (ter Braak and Šmilauer 2012).

Results

Inter-annual Changes in Water Quality

Water quality changes from 2018-2021

Monthly measurements of water quality parameters showed high temporal and spatial variability over the three years from 2018 to 2021 and among 6 sites, including salinity, water temperature, chlorophyll a, total nitrogen (TN), total phosphorus (TP), and total suspended solids (TSS) (Fig. 3-8). Most parameters showed pronounced seasonality. Salinity showed noticeable seasonality and spatial variability, showing, in general, lower at BB05a and BB01 and higher at BB07a. At BB07a, 1661A, and 1663A, salinity decreased by 4-8 ppt in the subsequent winter 2018 to early spring 2019, especially 1661A showed a salinity drop of 8 ppt, the largest of all three sites. The lowest temperature was detected in January-February while the highest in July-August, and the measurements were comparable among the sites. Water temperature below 0 ºC was detected just at BB01 in January 2020 (Fig. 4). Before the decommission, temperature at 1663A was generally higher than 1661A. After the first step of shutdown, the temperature became very similar between these two sites. At BB07a, there was about 4ºC temperature drop in October 2018 compared to other years (Fig. 10). However, a similar decrease in temperature was detected at both BB01 and BB09 in the same month. Chlorophyll *a* showed two peaks every year at most of sites, with first peak during winter between January-February and the second peak in summer between July and August. Spatially, the concentrations of chlorophyll *a* were higher at BB01 and BB05a and lower at BB09 and BB07a, contrary to salinity (Fig. 5). TN (Fig. 6) and TP (Fig. 7) showed similar trends as chlorophyll *a* in temporal and spatial distributions. TSS fluctuated through the years and high values were generally detected in winter. In general, TSS at BB09 was higher than other sites (Fig. 8). No noticeable short-term changes, separate from seasonality, in chlorophyll *a*, TN, TP and TSS were observed after the first step of decommissioning compared to previous years.

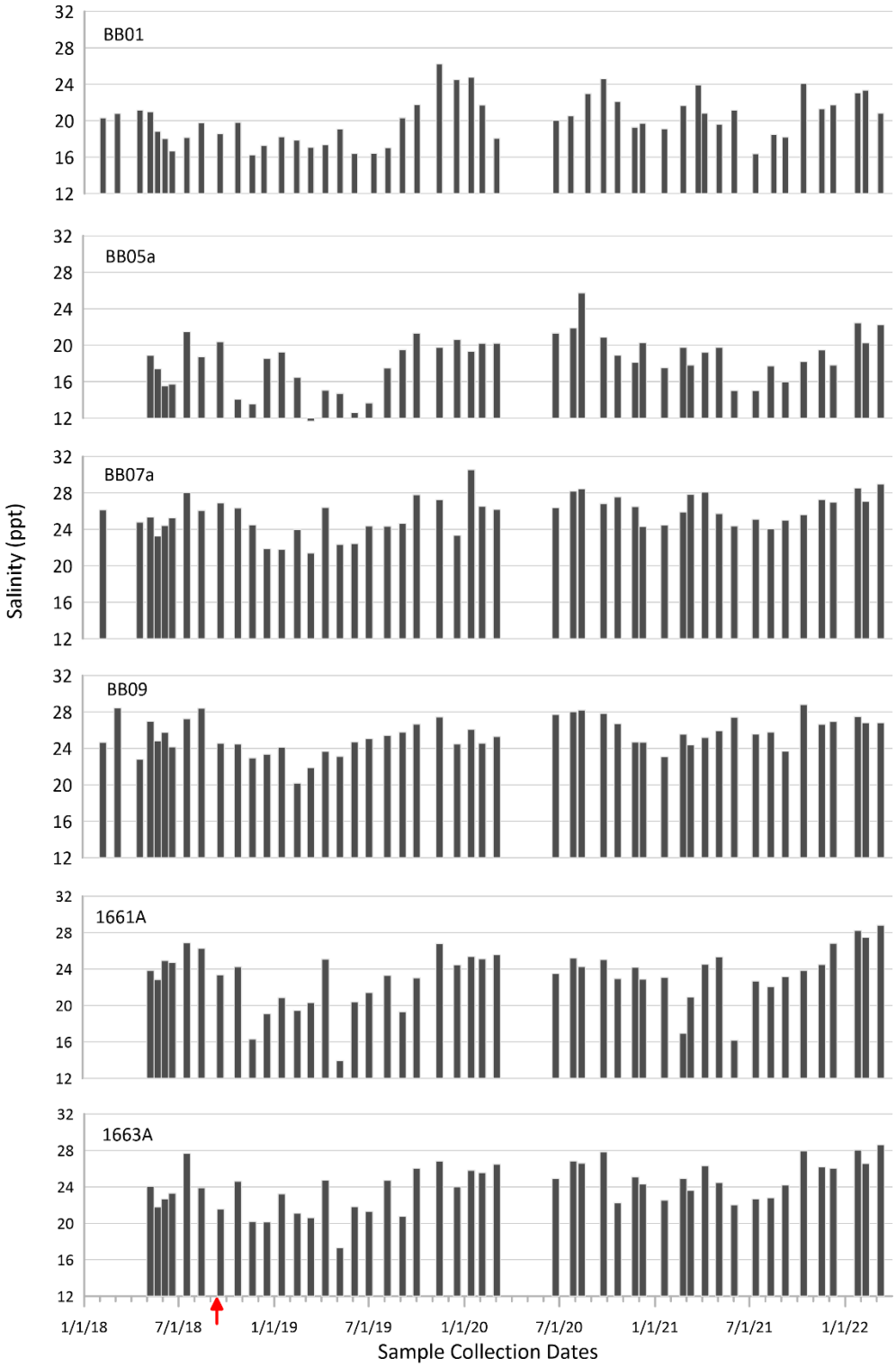

Fig. 3. Time series of salinity (ppt) from 2018-2021 at 6 sites in Barnegat Bay, BB01, BB05a, BB07a, BB09, 1661A and 1663A. Red arrow: the first closure of OCNGS, 9/17/2018.

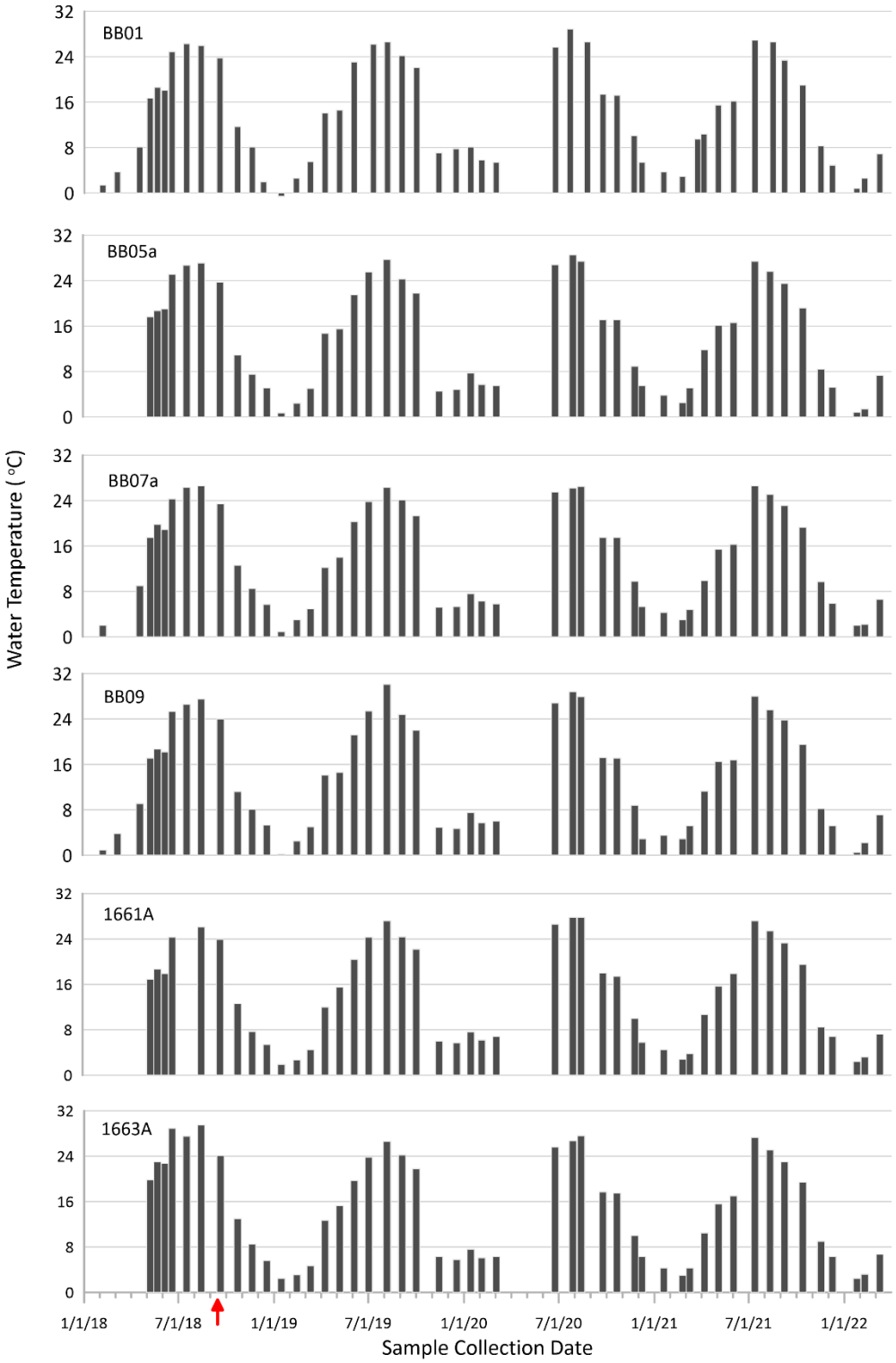

Fig. 4. Time series of water temperature (°C) from 2018-2021 at 6 sites in Barnegat Bay, BB01, BB05a, BB07a, BB09, 1661A and 1663A. Red arrow: the first closure of OCNGS, 9/17/2018.

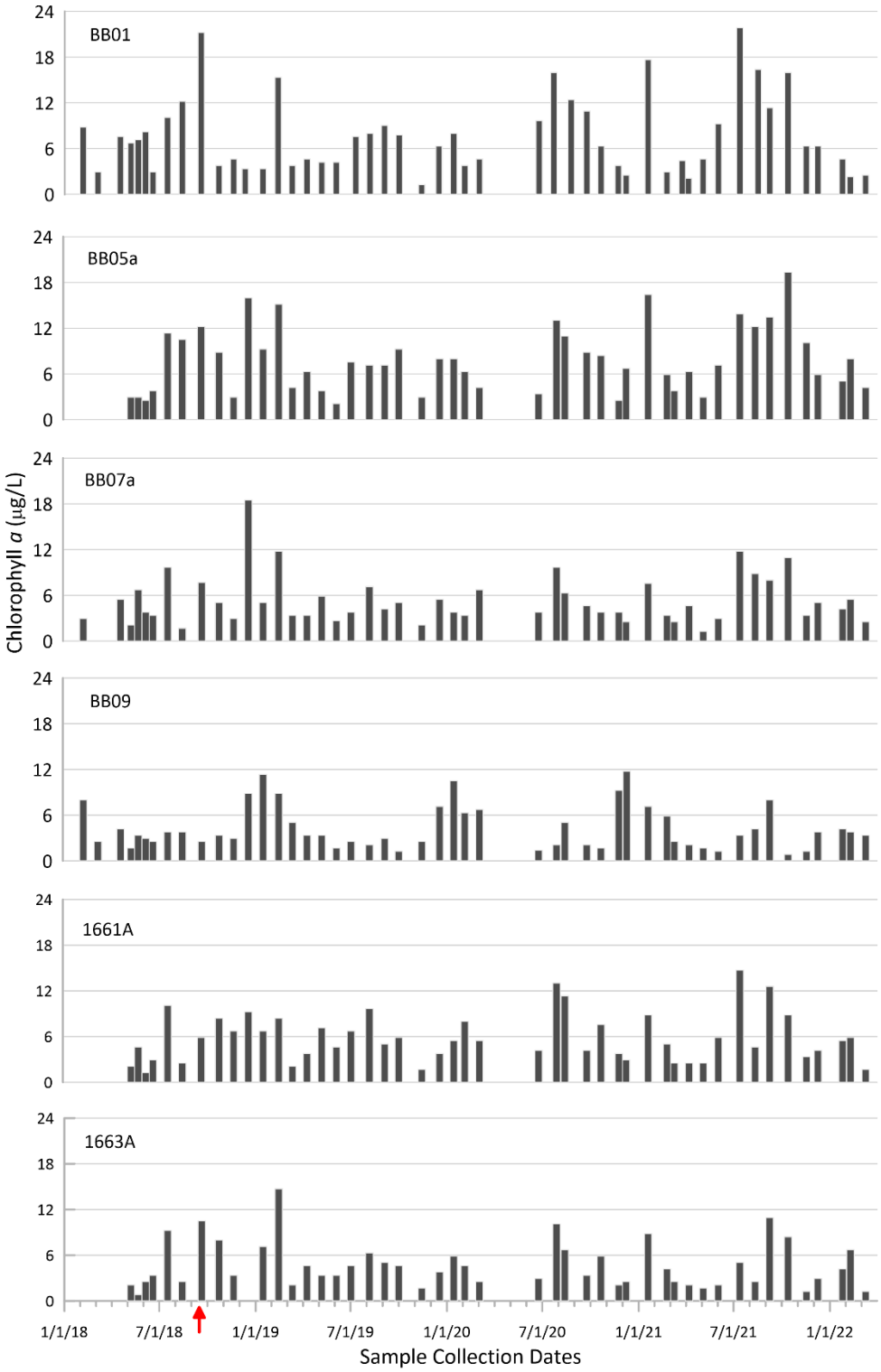

Fig. 5. Time series of Chlorophyll *a* (µg/L) from 2018-2021 at 6 sites in Barnegat Bay, BB01, BB05a, BB07a, BB09, 1661A and 1663A. Red arrow: the first closure of OCNGS, 9/17/2018.

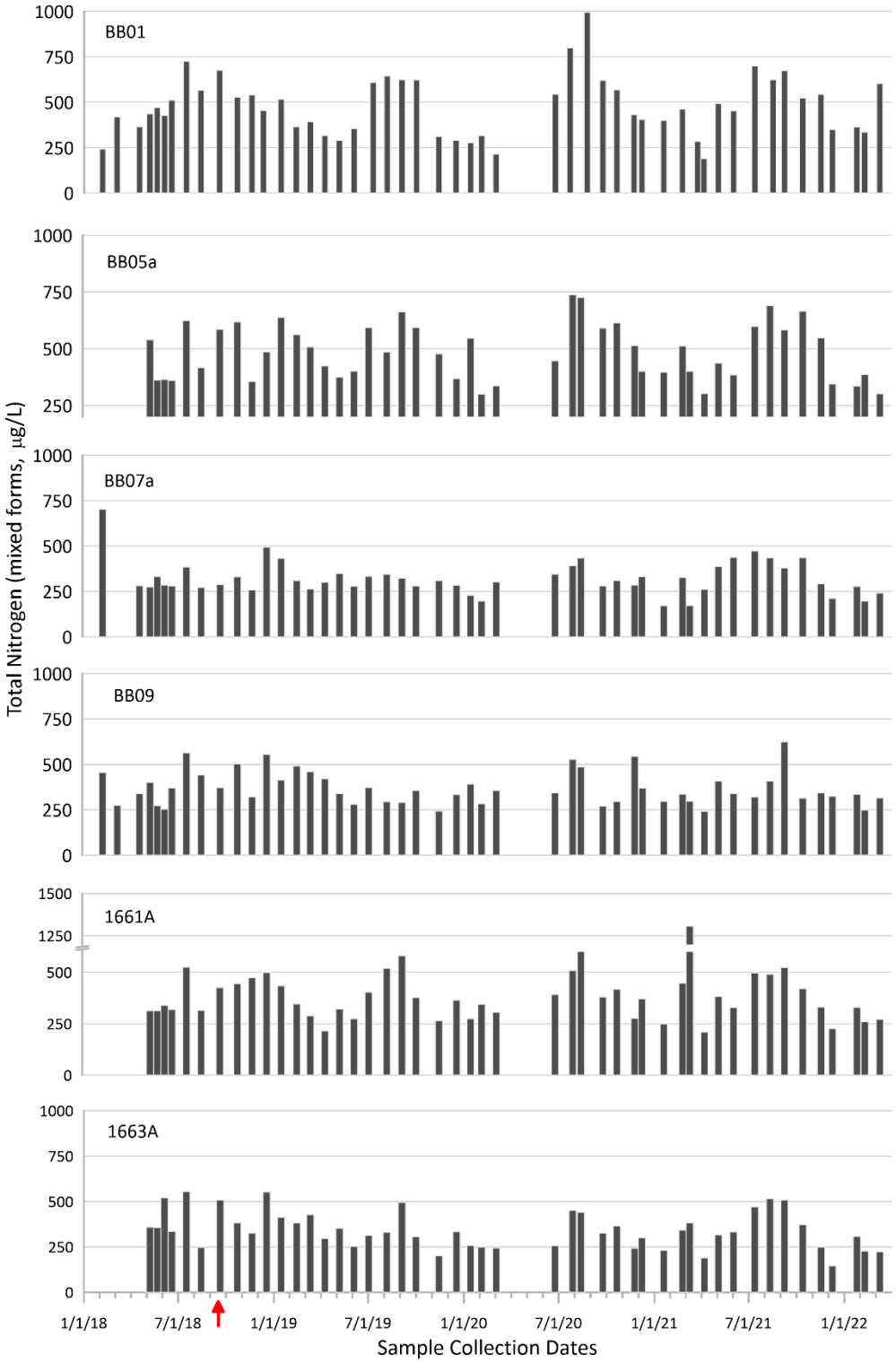

Fig. 6. Time series of total nitrogen (TN, µg/L) from 2018-2021 at 6 sites in Barnegat Bay, BB01, BB05a, BB07a, BB09, 1661A and 1663A. Red arrow: the first closure of OCNGS, 9/17/2018.

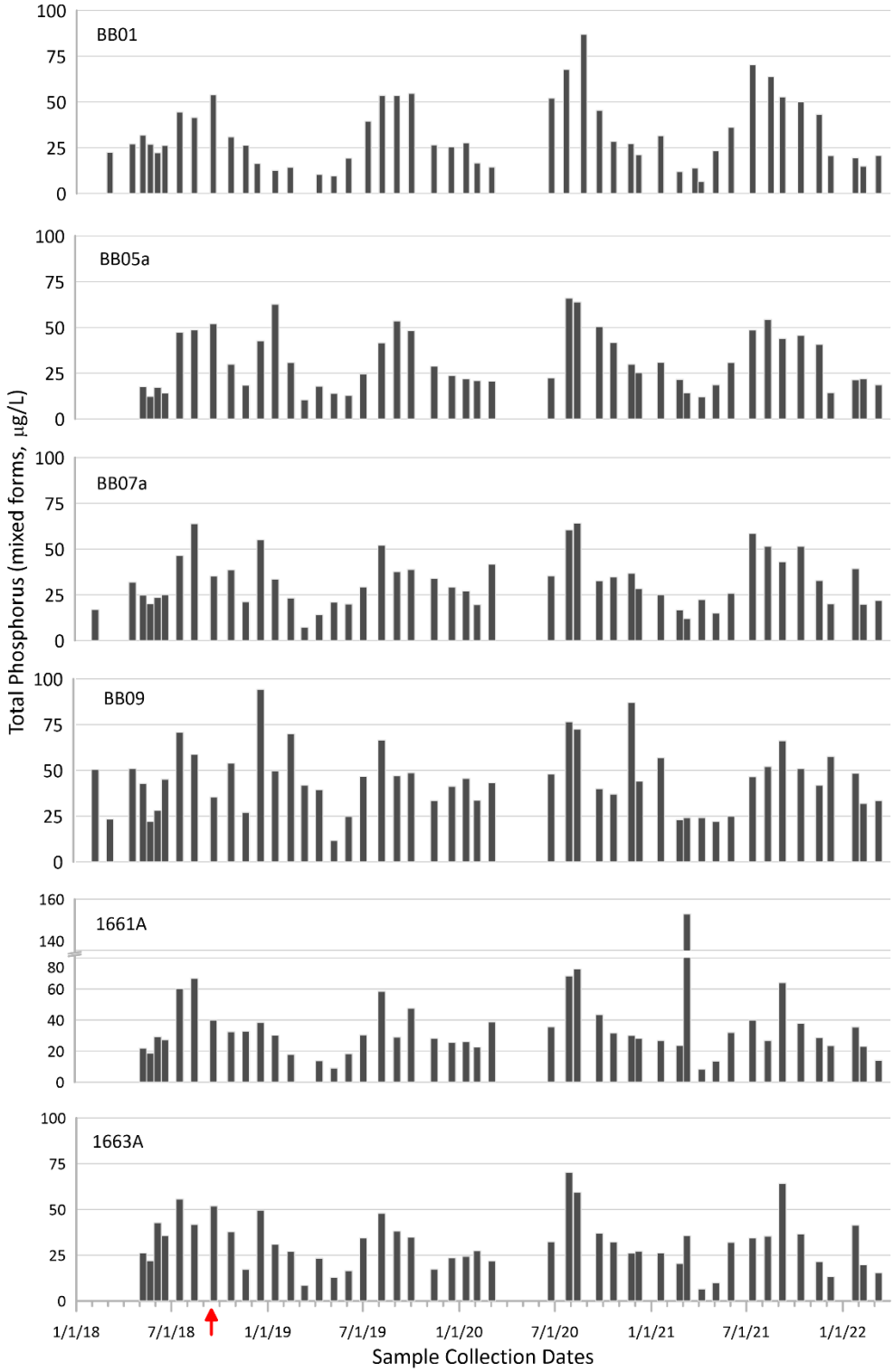

Fig. 7. Time series of total phosphorus (TP, µg/L) from 2018-2021 at 6 sites in Barnegat Bay, BB01, BB05a, BB07a, BB09, 1661A and 1663A. Red arrow: the first closure of OCNGS, 9/17/2018.

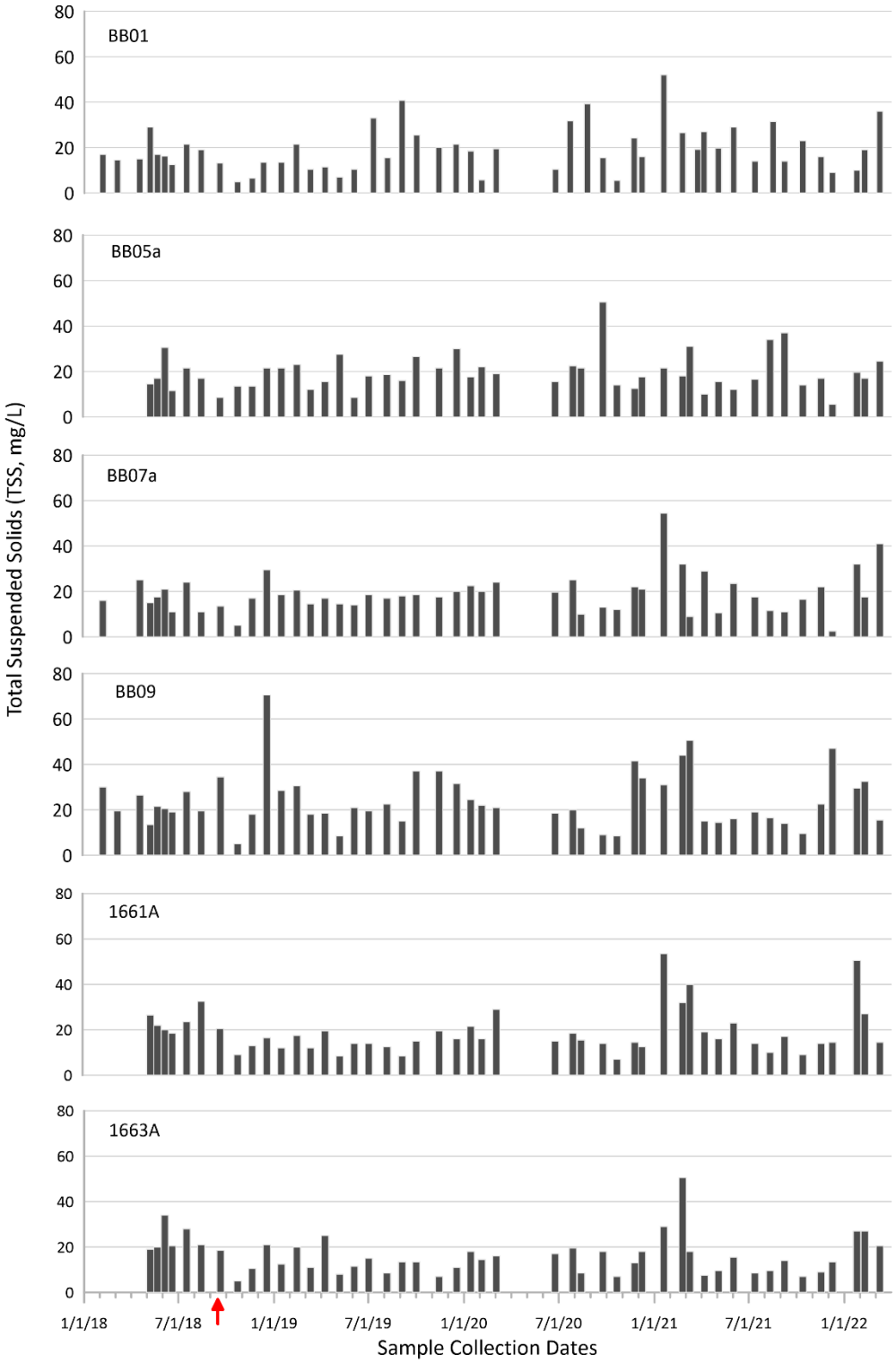

Fig. 8. Time series of total suspended solid (TSS, mg/L) from 2018-2021 at 6 sites in Barnegat Bay, BB01, BB05a, BB07a, BB09, 1661A and 1663A. Red arrow: the first closure of OCNGS, 9/17/2018.

Water quality changes from 2012-2021

In addition to water quality measurements from 2018-2021, measurements of the water quality parameters from 2012 to 2017 are plotted for the sites BB01, BB07a and BB09. Water temperature, salinity, total nitrogen (TN), and total phosphorus (TP) showed pronounced seasonal and year-to-year variations in the same month (Fig. 9-11).

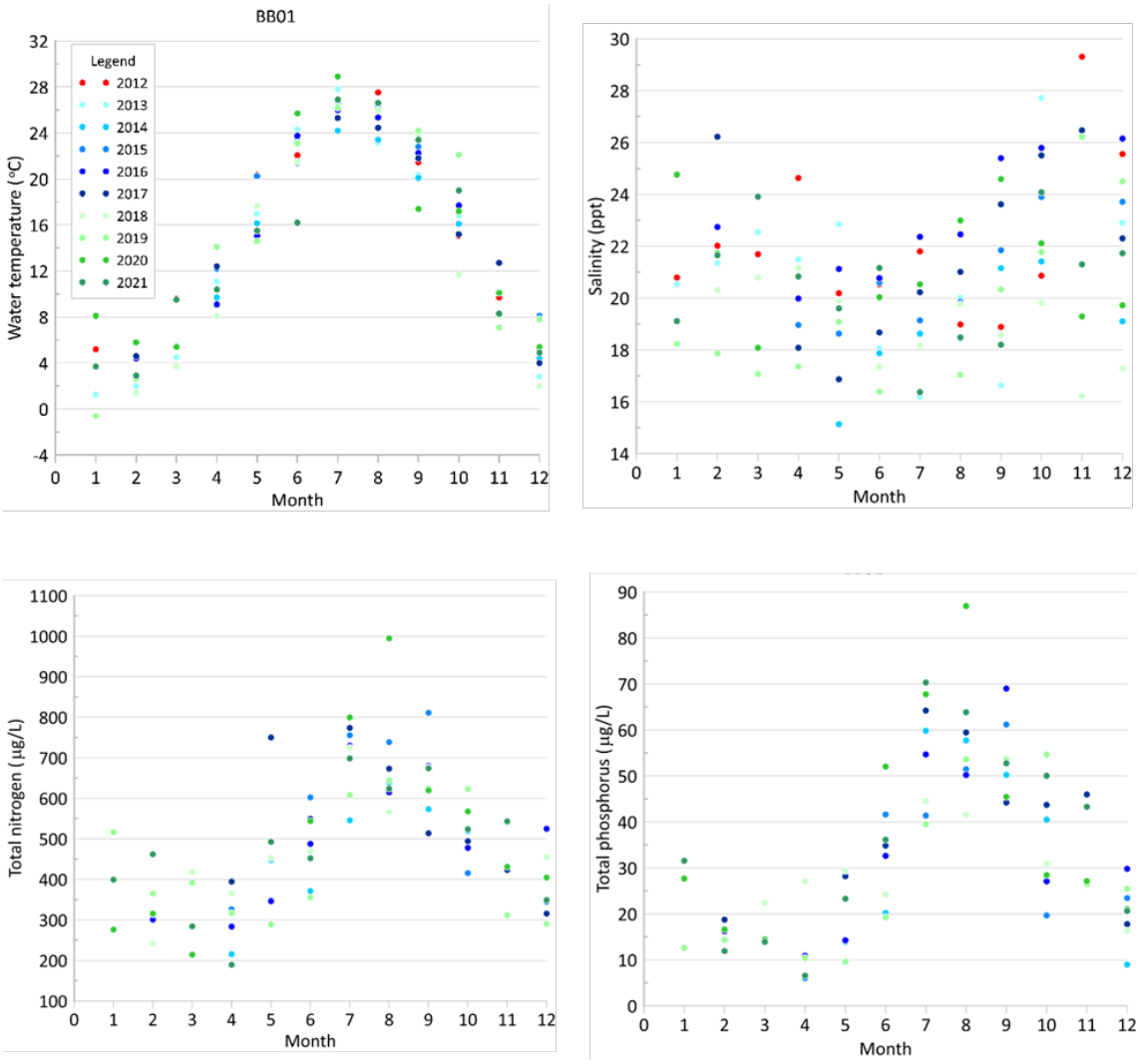

Fig. 9. Monthly and annual variability of water temperature, salinity, total nitrogen (TN), and total phosphorus (TP) at BB01 from 2014-2021 (salinity and temperature from 2012).

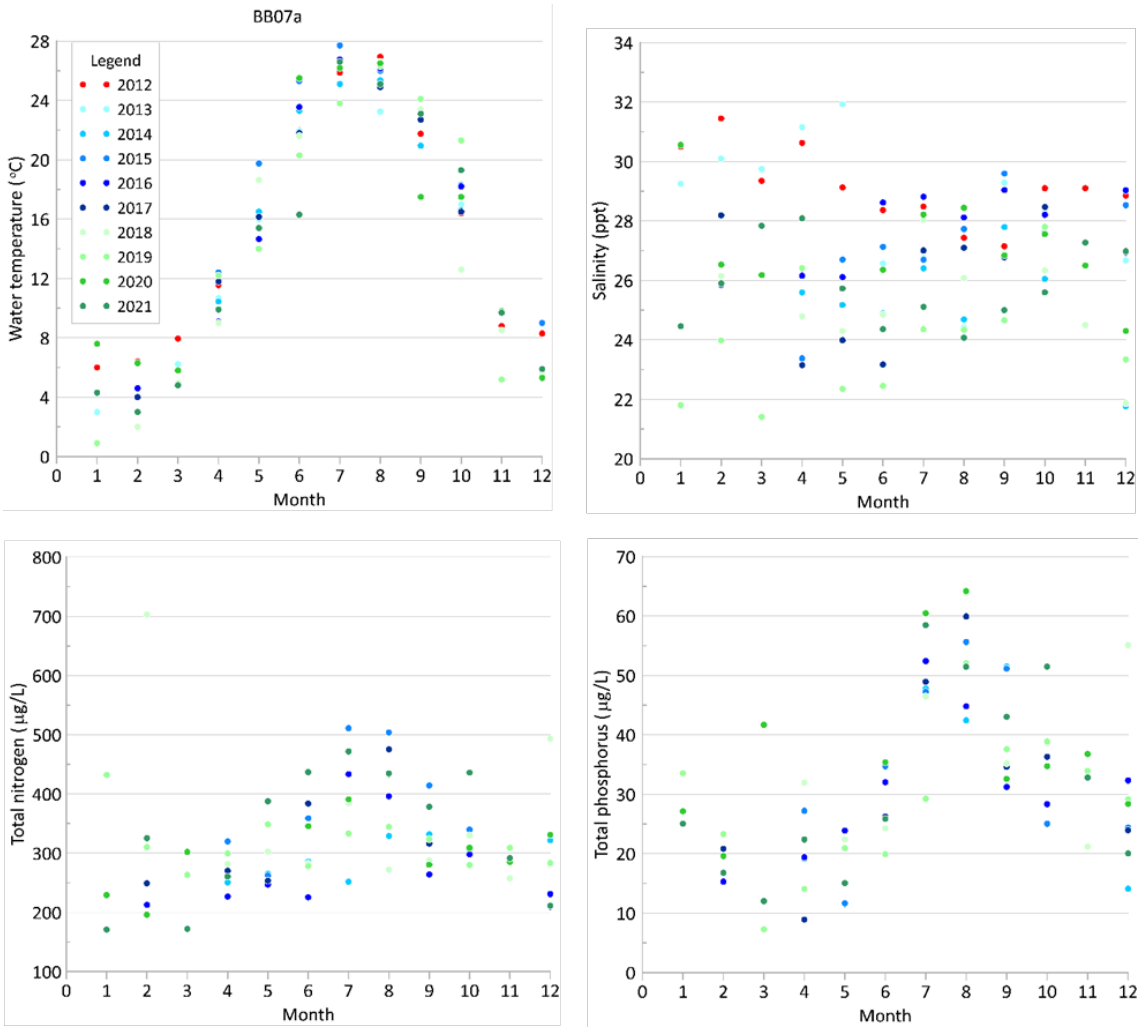

Fig. 10. Monthly and annual variability of water temperature, salinity, total nitrogen (TN), and total phosphorus (TP) at BB07a from 2014-2021 (salinity and temperature from 2012).

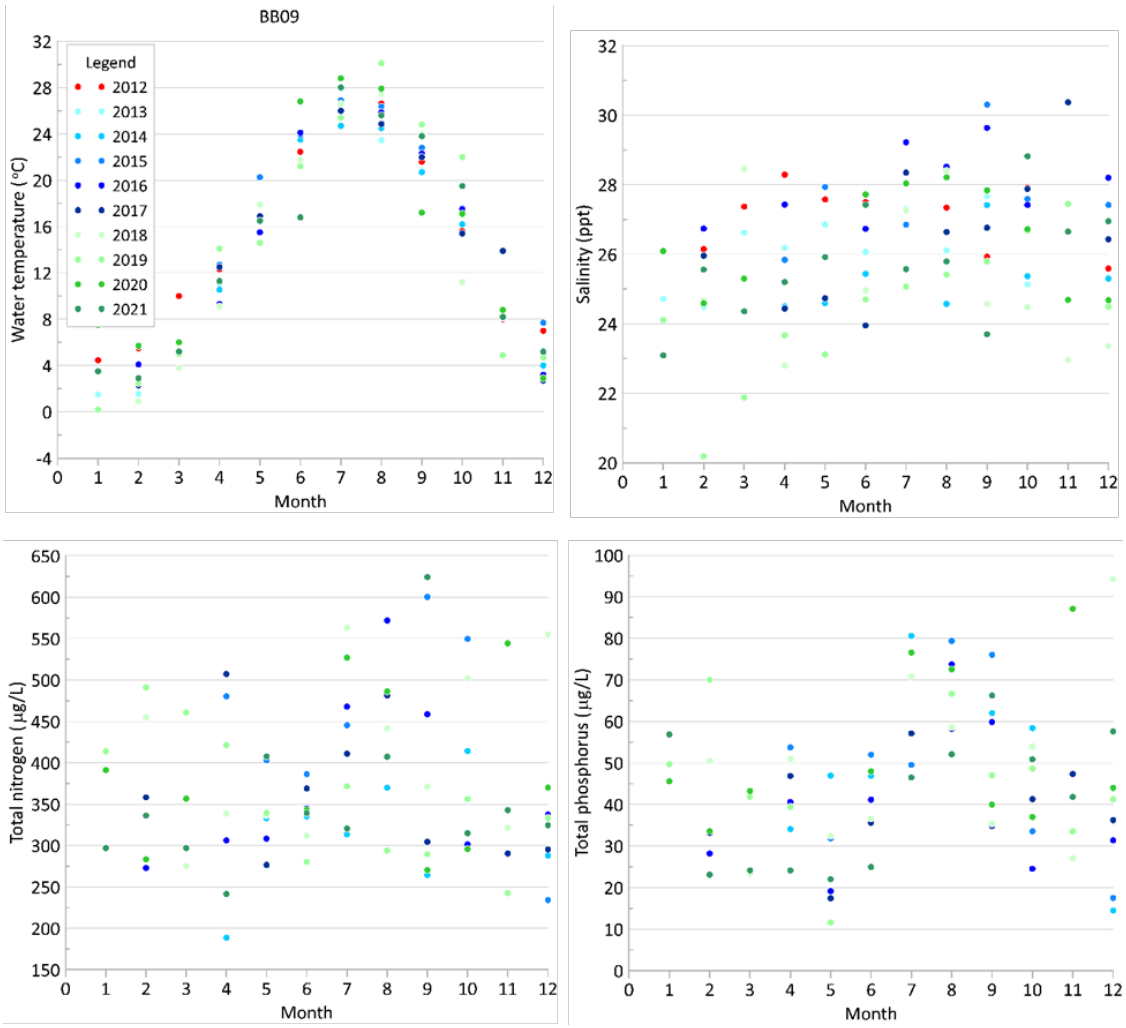

Fig. 11. Monthly and annual variability of water temperature, salinity, total nitrogen (TN), and total phosphorus (TP) at BB09 from 2014-2021 (salinity and temperature from 2012).

Correlations among environmental variables 2014-2021

PCA analysis was performed to investigate correlations between the environmental variables before and after the OCNGS closure at BB01, BB07a and BB09. The before-closure dataset contains the monthly/biweekly measurements from April 2014 to August 2018, and the after-closure dataset includes the measurements from September 2018 to December 2021.

PCA analysis showed that the correlations among environmental variables after the closure of the OCNGS varied from the 'before-closure' period.

At BB07a, nutrients, TN, TP, Ortho-P, were highly correlated to each other, and in strong positive relations to salinity before the closure (Fig. 12a), whereas after the closure, TN, TP, and Ortho-P were closely correlated to each other, but in weak and negative correlation to salinity (Fig. 12b). Biogenic silica (BSi) was closely correlated with dissolved oxygen (DO) but showed no correlation with chlorophyll *a* (ChlA) before the closure, however positively correlated with ChlA after the closure.

At BB01, nutrients were positively correlated to salinity before the closure, the correlation was not as strong as BB07a, judging from the angles between two parameters in the ordination diagrams (Fig. 13). TN and TP had a positive relationship to temperature (Fig. 13a). After the closure showed that Ortho-P and TP did not seem correlated to salinity, and TN showed a weak negative correlation with salinity (Fig. 13b). Both before- and after- closure data showed that ortho-P and TP were positively correlated to TSS, and chlorophyll *a* (ChlA) was positively correlated to nutrients (Fig. 13a, 13b).

At BB09, nutrients, particularly NH4, ortho-P, TN, and TP, were closely correlated, and in positive relationship with salinity before the closure (Fig. 13c). However, after the closure, bio-available nutrients, NH4 and ortho-P were closely correlated to each other but did not seem to correlate to salinity. TN and TP were also highly correlated to each other but in negative relationship to salinity (Fig. 13d). ChlA was highly correlated to BSi both before and after the closure, however, seemed to be little correlated to bioavailable nutrients, NH4 and ortho-P (Fig. 13c, 13c).

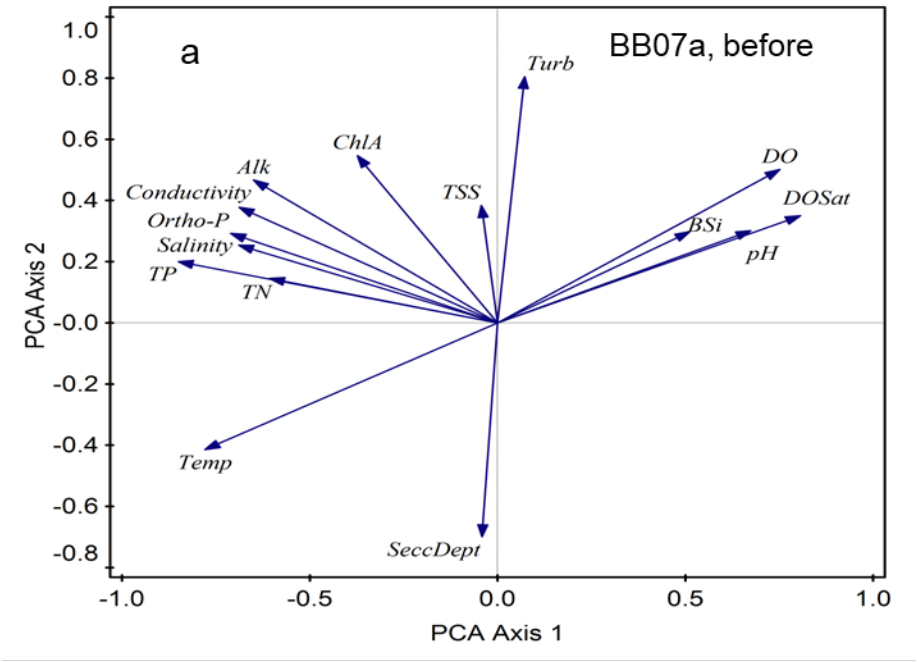

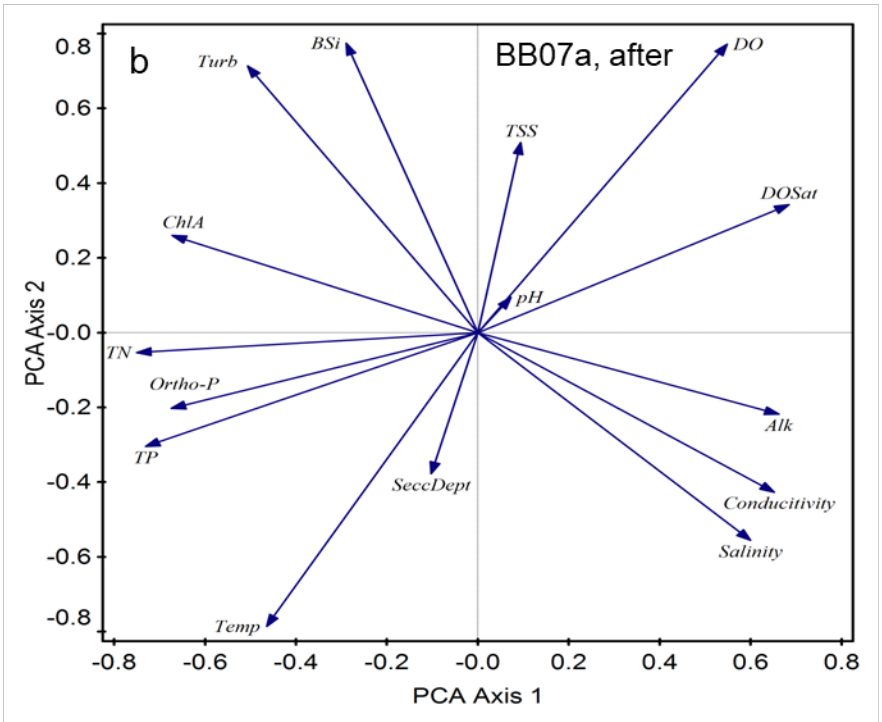

Fig. 12. Correlations of environmental variables derived from PCA at BB07a, before and after the closure of OCNGS. The ‘before’ dataset includes monthly data from April 2014 to August 2018; the ‘after’ dataset includes monthly data from September 2018 to December 2021.

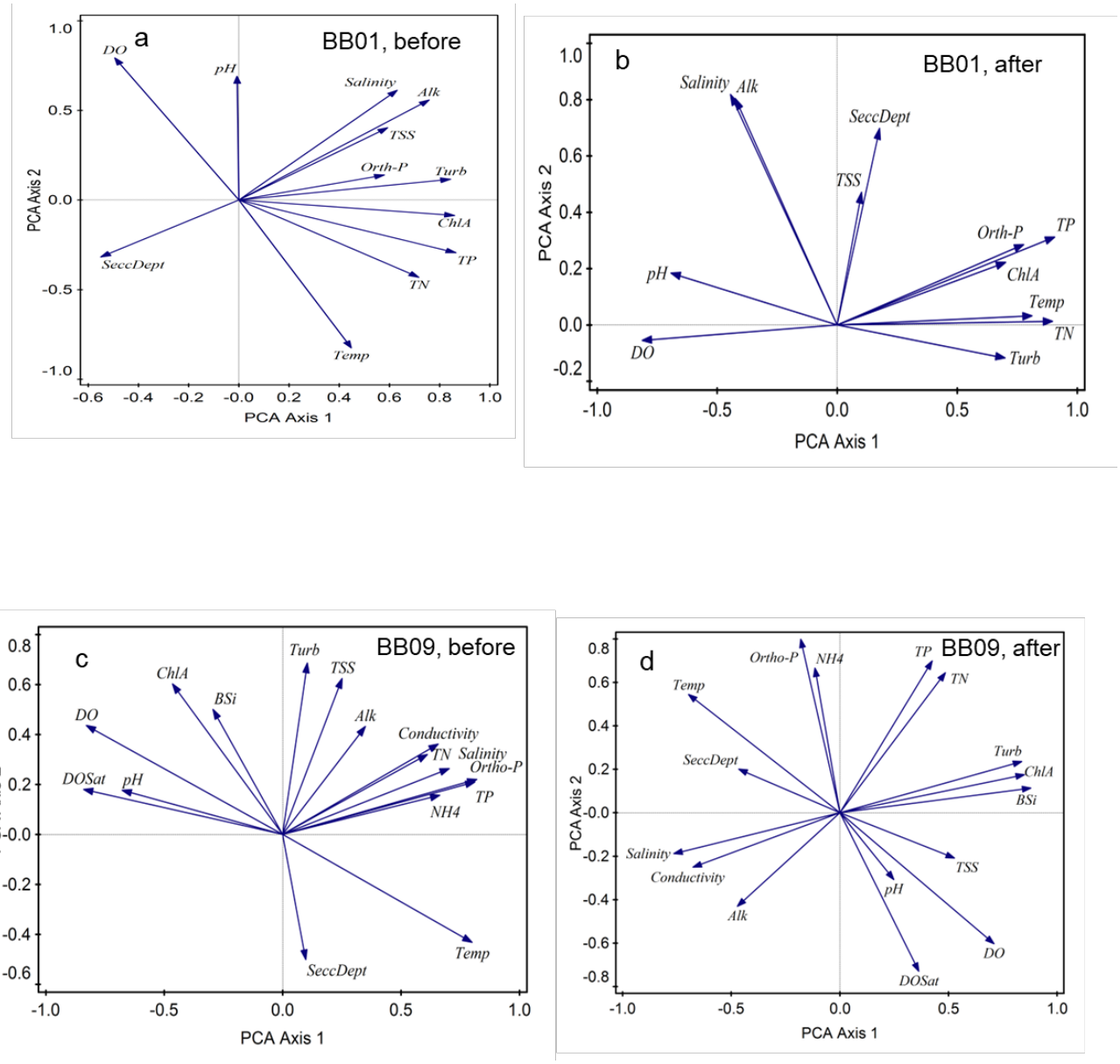

Fig. 13. Correlations of environmental variables derived from PCA at BB01 and BB09, before and after the closure of OCNGS. The 'before' dataset includes monthly data from April 2014 to August 2018; the 'after' dataset includes monthly data from September 2018 to December 2021.

Temporal and Spatial Changes of Phytoplankton

Temporal and spatial changes of phytoplankton, in terms of species composition and abundances, were characterized for the study period of 2018-2021, using the principal coordinates analysis (PCO) analyses based on microscopy and DNA data. In addition, for Barnegat Bay sites BB01, BB07a and BB09, a comparison was made between the 2018-2021 data and the dataset from 2014-2017 upon data availability. Both datasets were obtained using the same microscopic methodology for species identification and counting. Note that the DNA-based comparison was made at the level of classes/groups, and the microscopy-based comparison was done at the genus/species level, thus providing a deeper comparison of the composition shifts in terms of common and abundant genera/species.

Phytoplankton changes based on DNA sequences (2018-2021)

The changes of phytoplankton, in terms of the composition and abundances of classes and groups, were explored based on DNA data collected from sites BB01, BB05a, BB07a and BB09 between October 2017 and December 2021 (Fig. 14-17), and from sites1661A and 1663A between August 2018 and December 2021 (Fig. 18).

Phytoplankton community composition at the same site showed significant seasonality every year. The inter-annual variability of phytoplankton, over the three years, was generally overlapped by seasonality as shown by the mixed distributions of samples in the PCO ordination diagrams (Fig. 14-18). The characteristics of temporal variations varied between the sites. At BB01, the compositions of summer assemblages were comparable among the three years, as indicated by the aggregation of samples from June to September (BB01, Fig. 14, lower right quadrant; BB09). For the other months, phytoplankton community composition varied from year to year between 2018-2021. For instance, at BB01, February samples from 2019-2021 were close in the ordination diagram (Fig. 14), whereas January and March samples from those years were much further apart. At BB09, most samples from May to November of the three years were clustered together, whereas January to April samples were more scattered, showing monthly and year-to-year variations (Fig. 17).

At BB07a, most January-April samples were generally comparable over the years of 2018-2021, so were the July-September and the October-December ones. The May-June samples were more scattered showing larger variability in monthly as well as year-to-year changes. In general, the spring and fall samples showed higher month-to-month variations when the temperature varies the most. Comparing the August and October samples, the difference in 2018 was smaller than that in 2019, but larger than 2021 (Fig. 16).

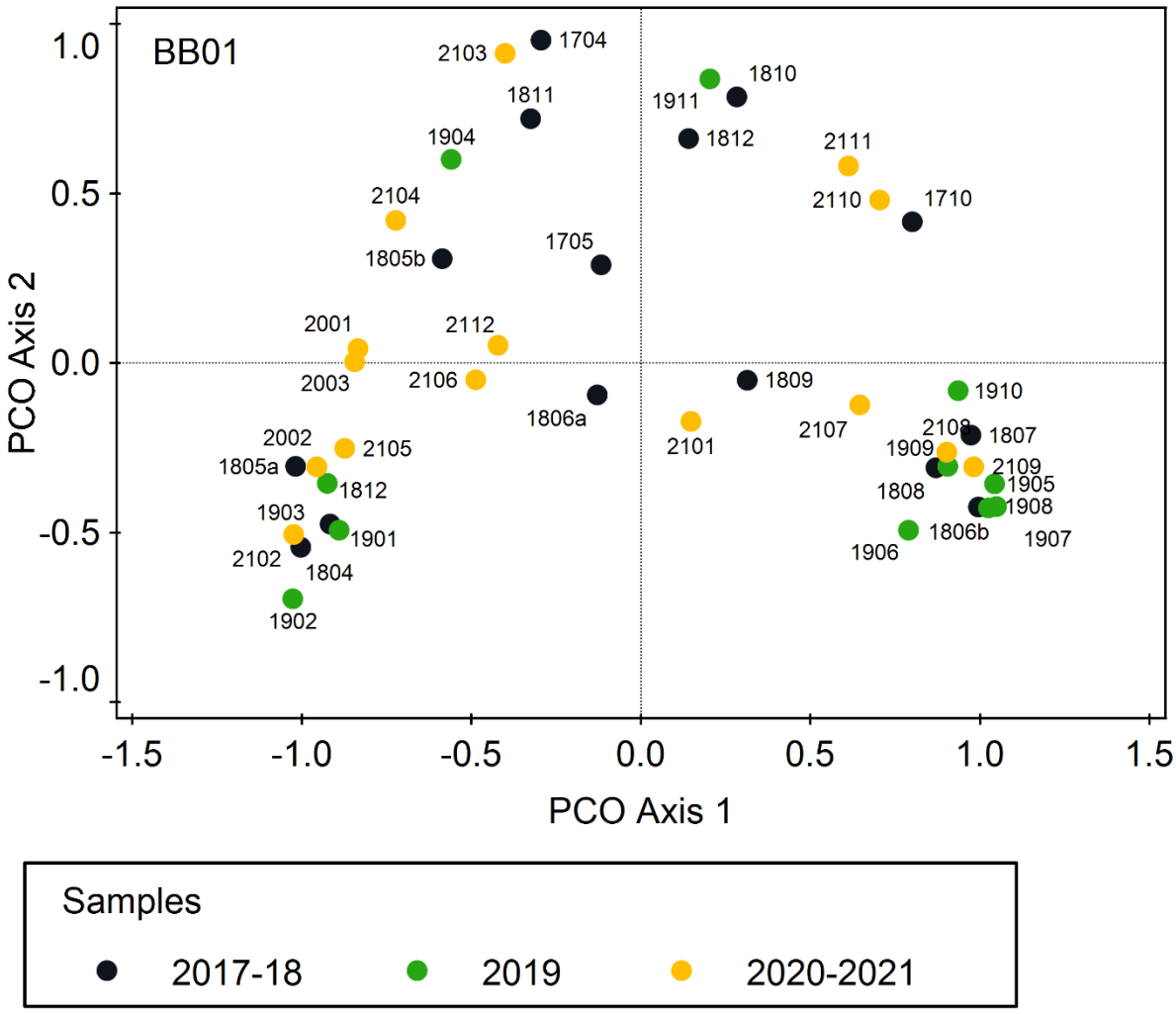

Fig. 14. Inter-annual variations of phytoplankton at BB01 from 2018-2021, based on DNA sequence data. Note: samples were collected monthly from April to December in 2018, January to December in 2019 and 2021, and additionally, from April, May and October in 2017, and January to March in 2020. Dots represent samples which are labelled with collection year and month (YYMM).

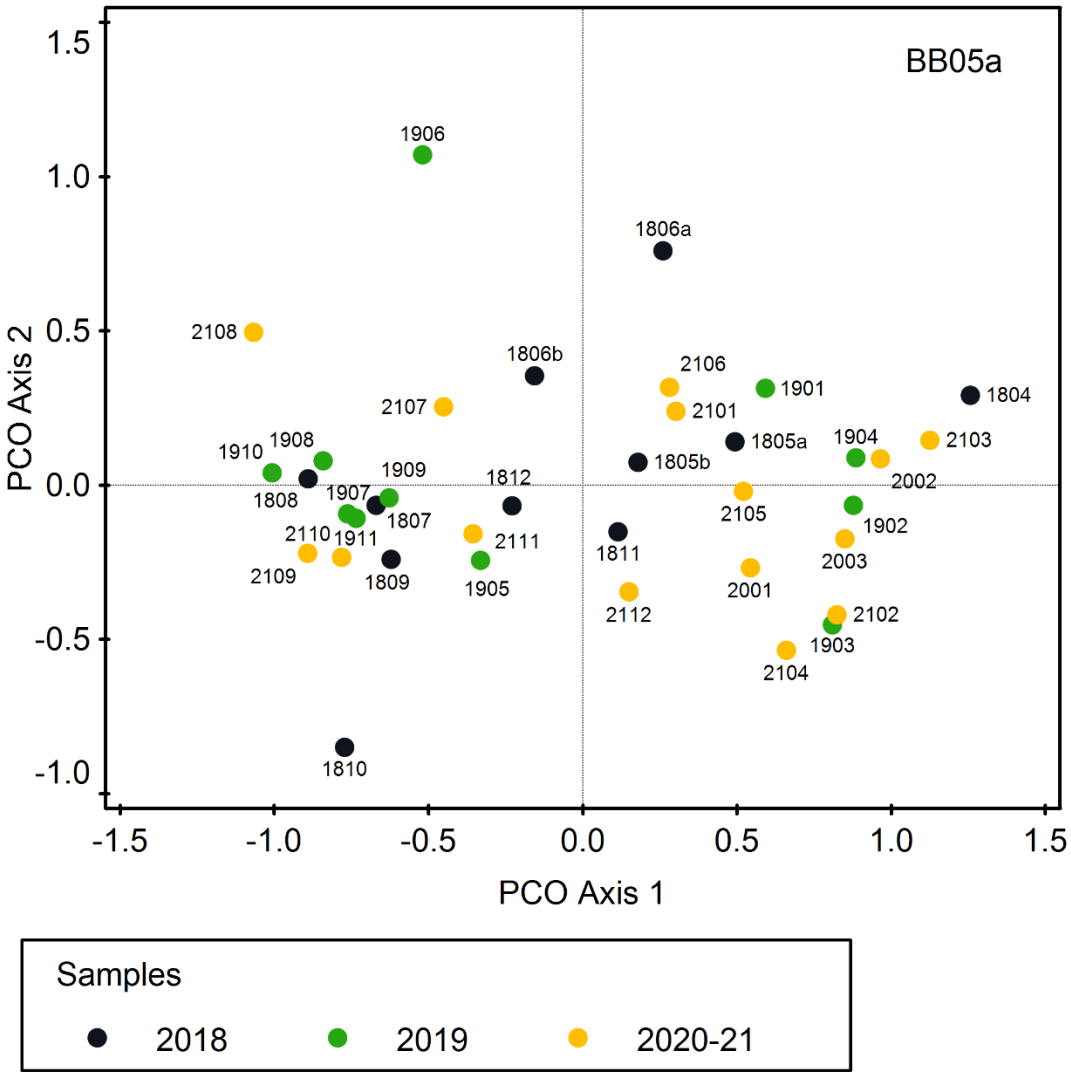

Fig. 15. Inter-annual variations of phytoplankton at BB05a from 2018-2021, based on DNA sequence data. Note: samples were collected monthly from April to December in 2018, January to December in 2019 and 2021, and January to March in 2020. Dots represent samples which are labelled with collection year and month (YYMM).

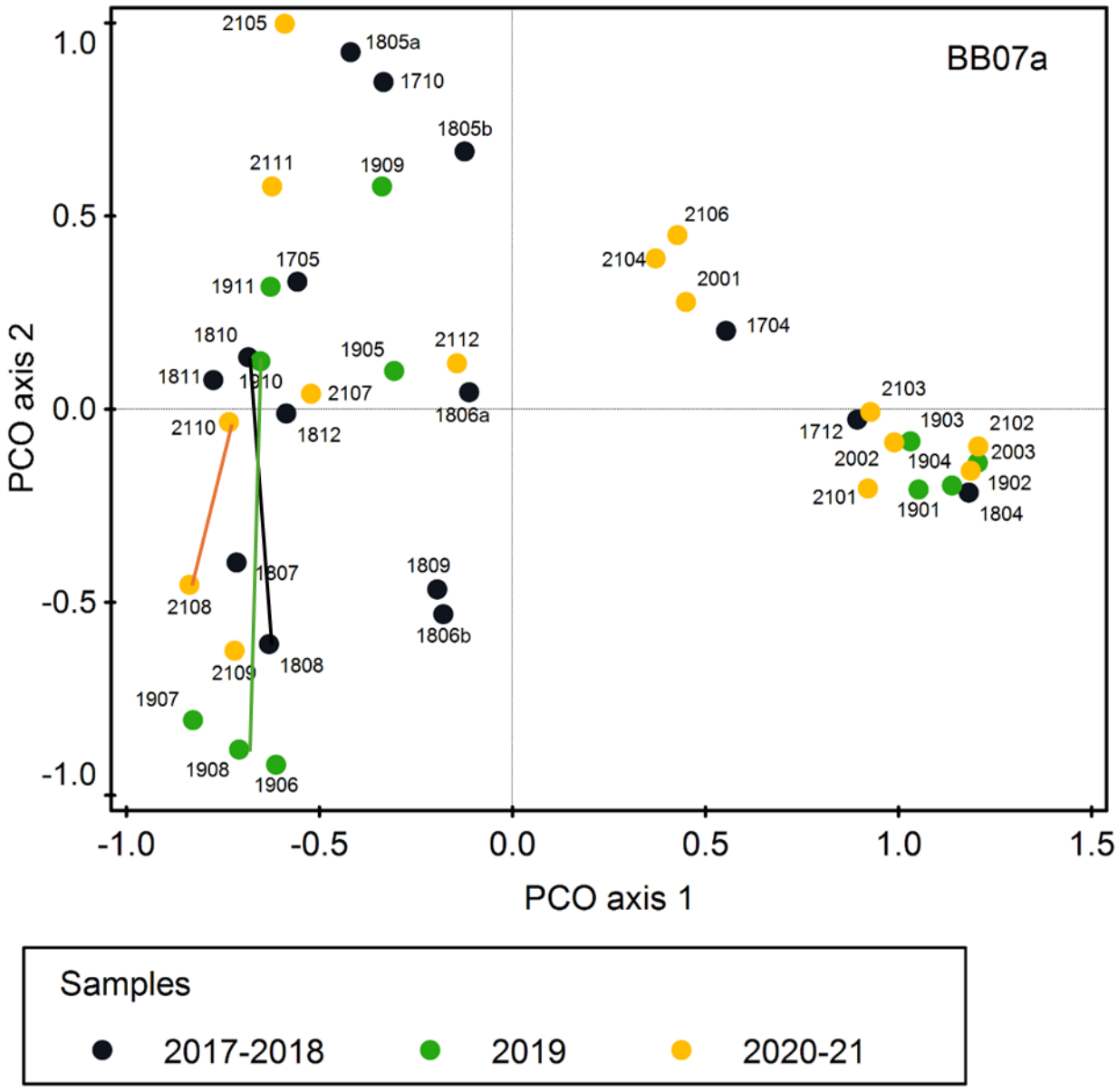

Fig. 16. Inter-annual variations of phytoplankton at BB07a from 2018-2021, based on DNA sequence data. Note: samples were collected monthly from April to December in 2018, January to December in 2019 and 2021, and additionally, from April, May, and October in 2017, and January to March in 2020. Dots represent samples which are labelled with collection year and month (YYMM).

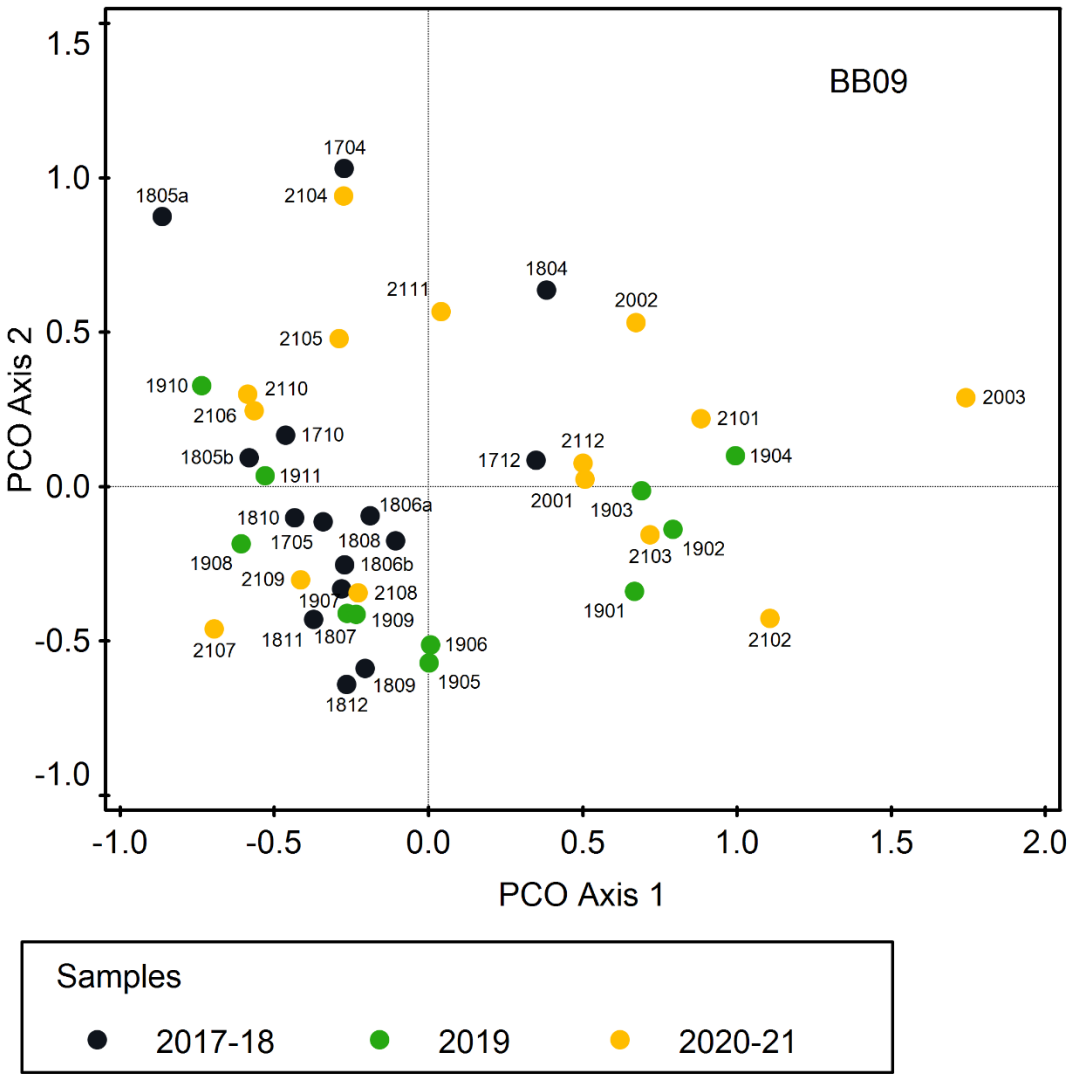

Fig. 17. Inter-annual variations of phytoplankton at BB09 from 2018-2021, based on DNA sequence data. Note: samples were collected monthly from April to December in 2018, January to December in 2019 and 2021, and additionally, from April, May and October in 2017, and January to March in 2020. Dots represent samples which are labelled with collection year and month (YYMM).

At site 1661A, the August 2018 sample, collected before the first shutdown of OCNGS, showed large differences from the other 2018 samples collected at 1661A, and there was large dissimilarity between the October and November 2018 samples. The August 2018 sample was much different from the August samples of 2019 and 2021, when the latter two were more similar. Moreover, for each month from October to December, the differences between 2018 and 2019 were larger than those between 2019 to 2021. However, the differences between August and October in 2021 were comparable to that in 2018. Moreover, some monthly variations, such as from February to March 2019, and from March to April 2021 were larger than those between August and October 2018, as indicated by the distances between samples in PCO ordination diagrams (Fig. 18a).

At 1663A, similar to 1661A, the August samples showed large differences from the other 2018 samples, and large dissimilarity was detected between the October and November 2018 samples. The differences between August and October 2018 were less than those in 2019 and 2021. The inter-annual differences of August samples were comparable between 2018, 2019 and 2021. The October community showed more similarity between 2018 and 2021 but varied from 2019, whereas November 2018 sample was very dissimilar from November 2019 and 2021 (Fig. 18b).

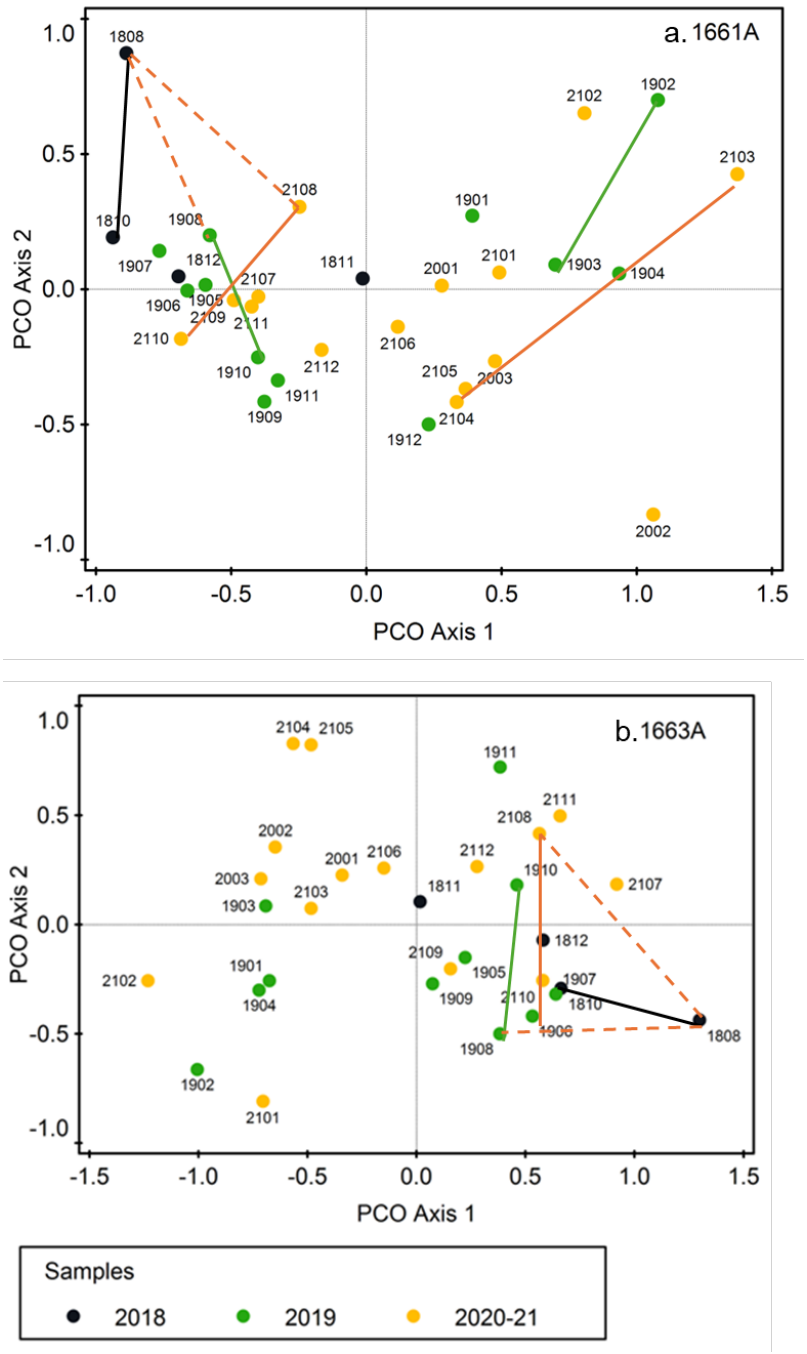

Fig. 18. Inter-annual variations of phytoplankton at sites 1661A and 1663A from 2018-2021, based on DNA sequence data. Note: samples were collected in August, October, and November in 2018, monthly from January to December in 2019 and 2021, and in addition January to March in 2020. Dots represent samples which are labelled with collection year and month (YYMM).

Phytoplankton changes based on microscopic analyses (2014-2021)

Microscopic data from 2018 to 2021 were compared with that from 2014 to 2017, to investigate long-term variations of phytoplankton at BB01, BB07a and BB09 (Fig. 19-21). Within each year, the seasonality of phytoplankton changes was noticeable at all three sites, consistent with DNA-based data from 2018-2021. Three-year (2018-2021) samples from this study were overall mixed with 2014-2017 samples in ordination diagrams, though year-to-year variability was noticeable at BB01 (Fig. 19) and BB09 (Fig. 21), judging from the sample distances. At BB07a, summer and fall assemblages were more comparable whereas winter and spring ones were more varied from year to year (Fig. 20). The degree of inter-annual changes at each site varied with different months. For summer months phytoplankton communities were more comparable between most years, whereas for the other months phytoplankton exhibited more variations from year to year. Monthly and seasonal shifts in phytoplankton composition could be as high as the year-to-year variations, or higher. These results are consistent with the DNA-based comparisons (Fig. 14, 16, 17).

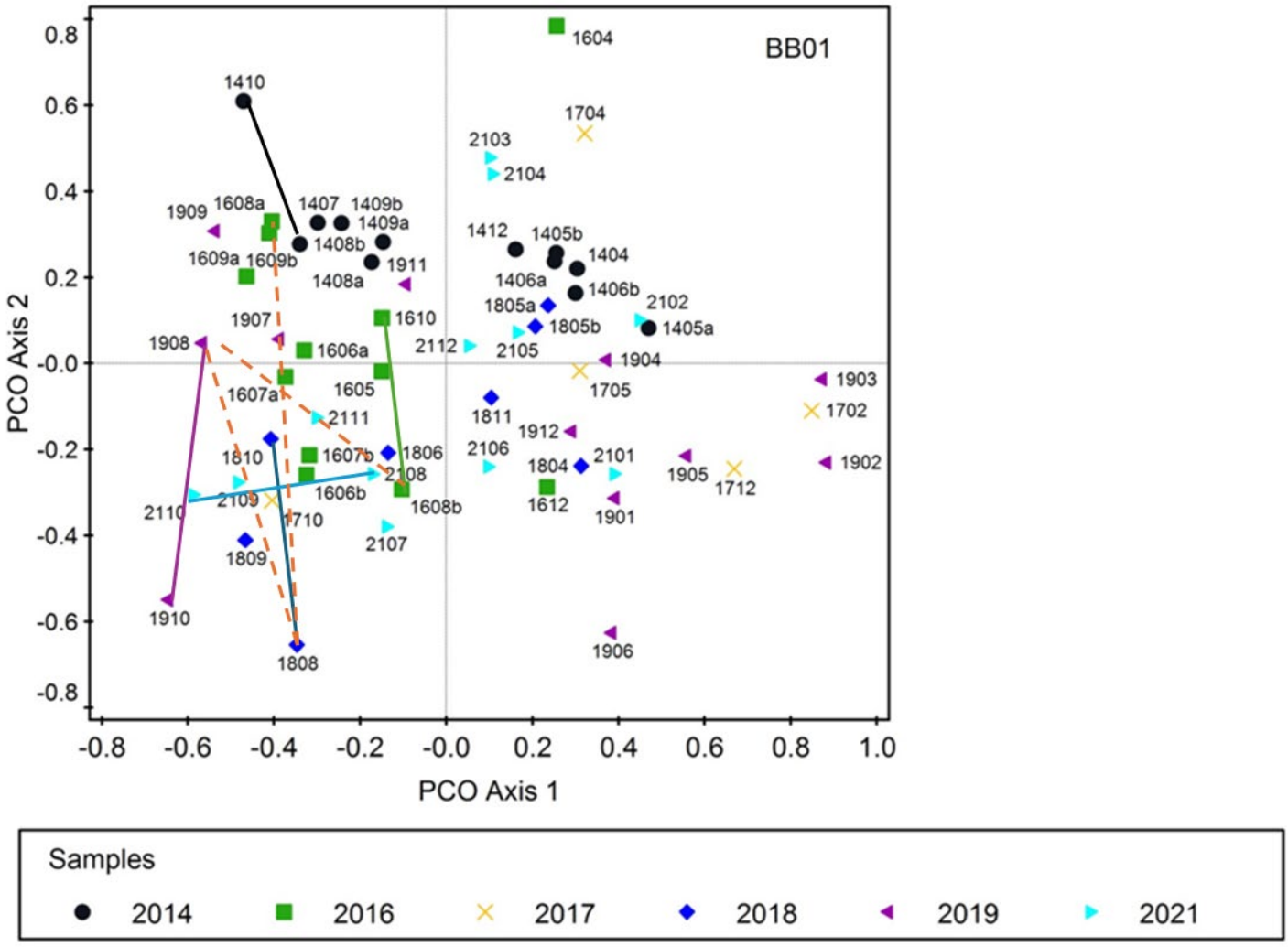

Fig. 19. Inter-annual variations of phytoplankton at BB01 from 2014-2021, based on microscopy data, diagram derived from Principal Coordination (PCO) analysis. Each dot represents one sample and is labelled as YYMM. Solid lines are dissimilarities August/October for same year; Dotted line are dissimilarities for August samples in different years.

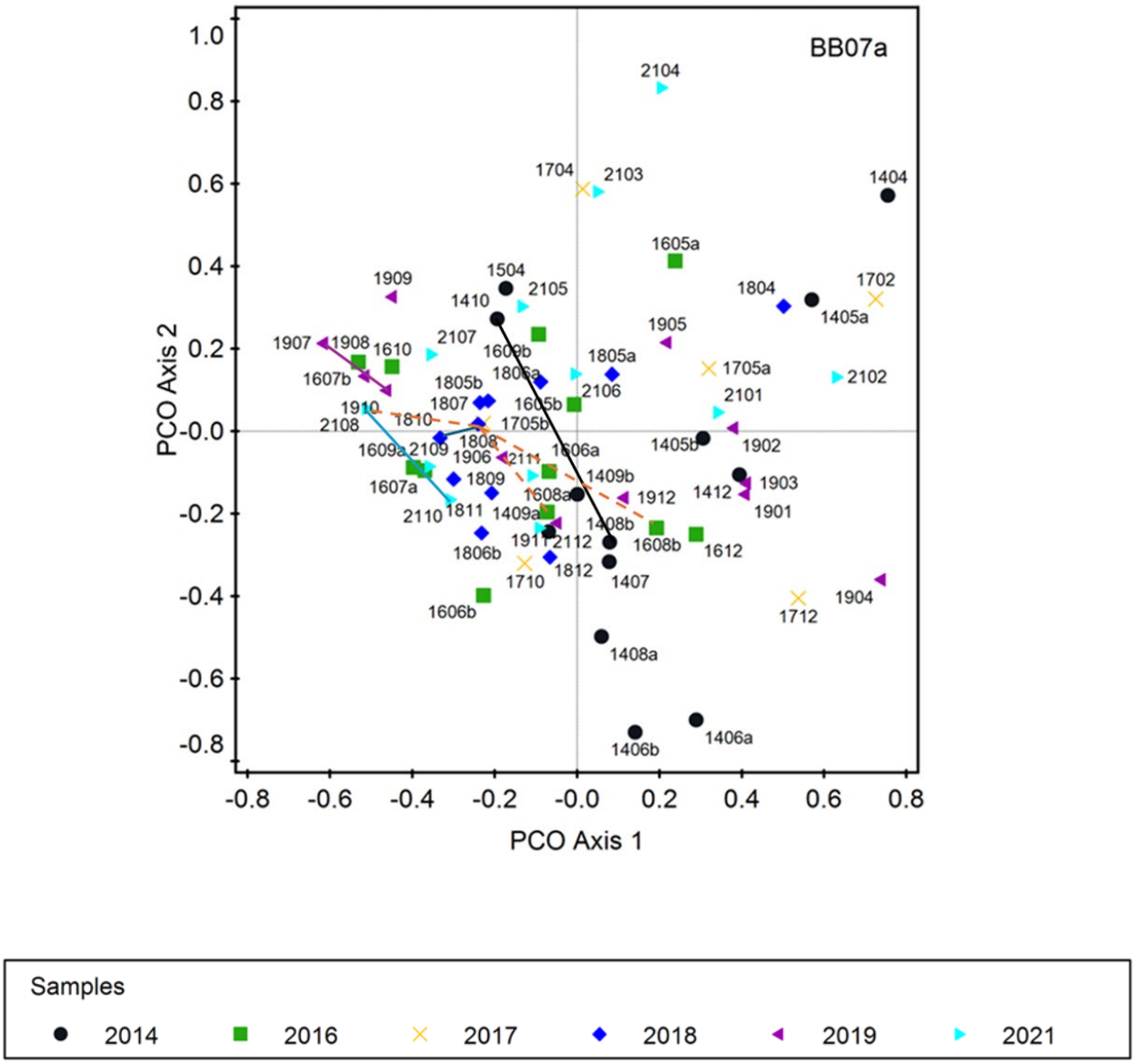

Fig. 20. Inter-annual variations of phytoplankton at BB07a from 2014-2021, based on microscopy data, diagram derived from Principal Coordination (PCO) analysis. Each dot represents one sample and is labelled as YYMM. Solid lines are dissimilarities August/October for same year; Dotted line are dissimilarities for August samples in different years.

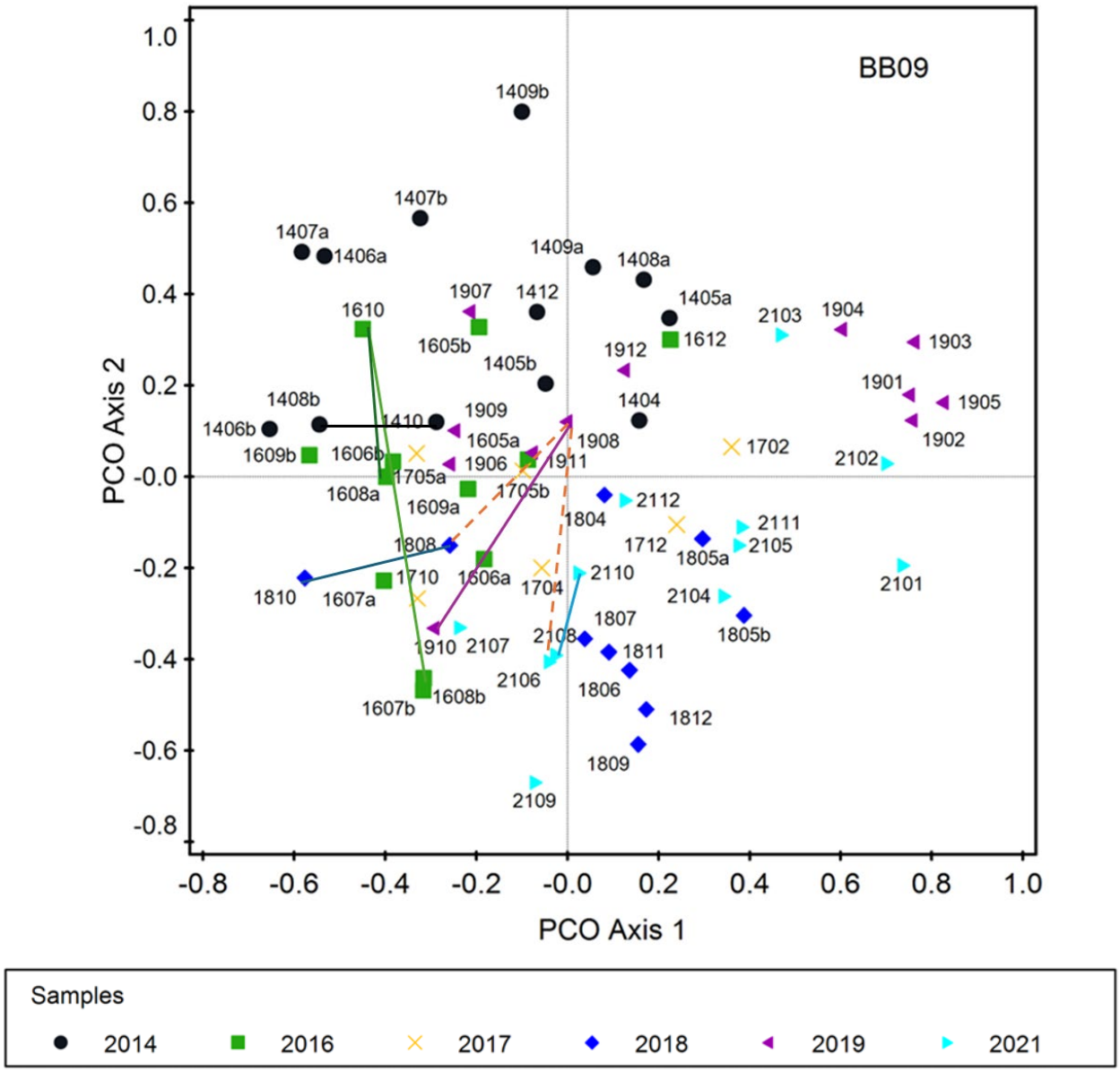

Fig. 21. Inter-annual variations of phytoplankton at BB09 from 2014-2021, based on microscopy data, diagram derived from Principal Coordination (PCO) analysis. Each dot represents one sample and is labelled as YYMM. Solid lines are dissimilarities August/October for same year; Dotted line are dissimilarities for August samples in different years.

Comparisons of Phytoplankton Before- and After-Closure

Phytoplankton changes at BB07a, 1661A and 1663A

To investigate the impact of OCNGS closure, samples collected at BB07a from the months of August, September, and October between 2012-2021 were pulled together and the microscopy-based phytoplankton communities were compared using PCO analysis. The analysis showed prominent changes in phytoplankton from August to October in 2018 in comparison to 2019 and 2021 (Fig. 22). Additionally, Table 3 presents the distances between pairs of samples derived from PCO analysis, comparing phytoplankton in the same month but different years. The results showed the highest variability of the August samples between the years 2012 vs. 2013, and 2018 vs. 2019. For the September samples, the largest dissimilarity (distance) was detected from 2018 vs. 2019. And the October samples had higher distance from 2018 vs. 2019, following 2014 vs. 2016 (Table 3).

Table 3: The distances between the samples at BB07a, derived from PCO analysis. The values approximate the dissimilarity/similarity of sample score values as measured by the Euclidean distance. The higher the distance values indicate less similarity (more dissimilarity) in phytoplankton compositions. Nd: no data.

Years	August	September	October
2012 vs 2013	0.61	nd	nd
2013 vs 2014	0.48	nd	nd
2014 vs 2016	0.48	0.52	0.61
2016 vs 2018	0.47	0.41	0.49
2018 vs 2019	0.56	0.54	0.59
2019 vs 2021	0.4	0.49	0.52

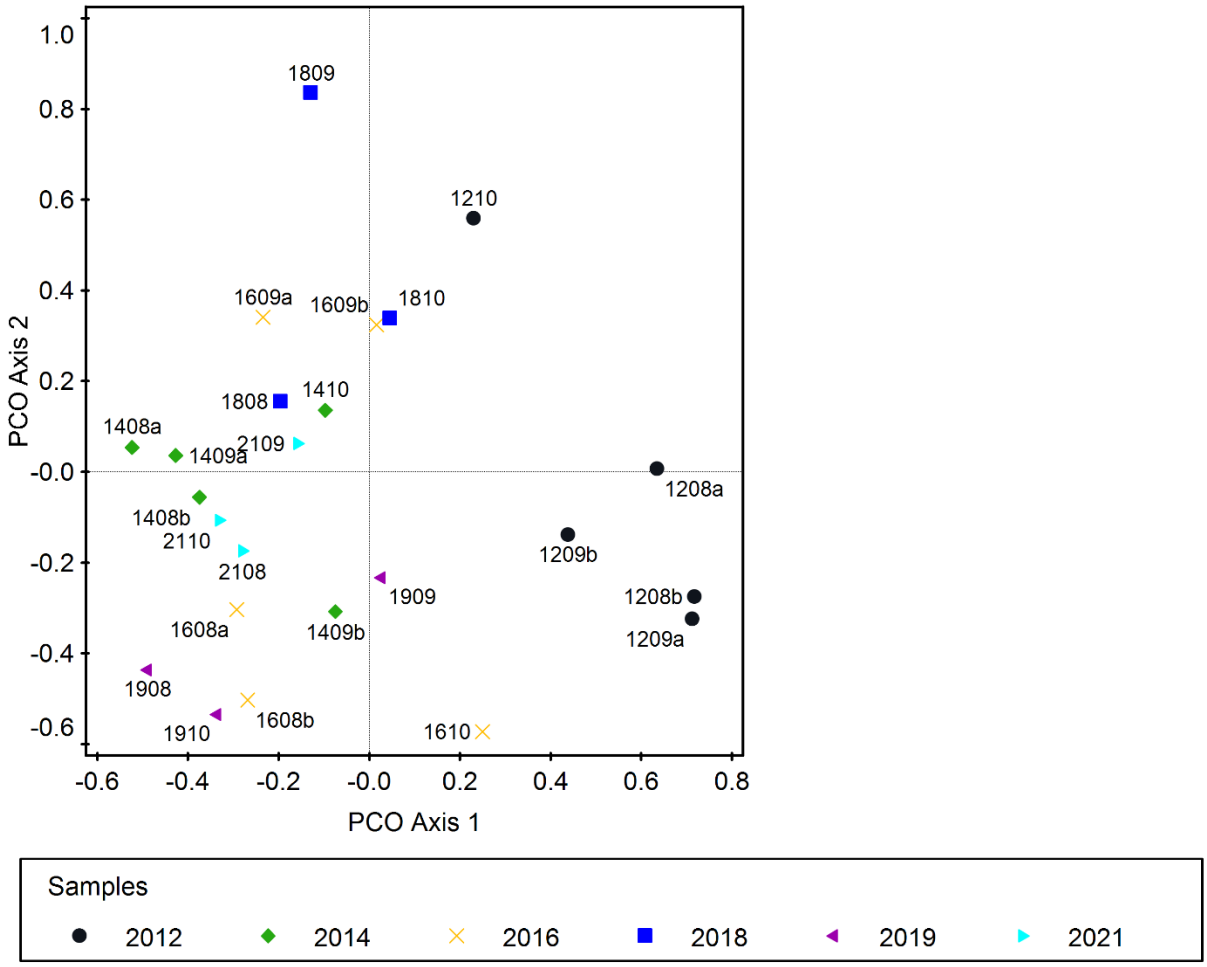

Fig. 22. Comparison of the August, September, and October phytoplankton compositions collected at BB07a from 2012 to 2021. Each dot represents one sample and is labelled as YYMM. The decommission of OCNGS started from the week of September 17, 2018.

In addition, the differences of phytoplankton between sites 1661A and 1663A were examined for each month using DNA data. PCO analysis showed that phytoplankton communities between these two sites exhibited the largest difference in August 2018 before the closure of OCNGS. After the first shutdown in September 2018, phytoplankton became more similar between the two sites in October and December 2018, though less similar in November. Subsequently, Phytoplankton remained comparable for most months in 2019 and 2021, except for September 2019 when distance between 1661A and 1663A was larger than that in August 2018, indicating larger dissimilarity (Fig. 23).

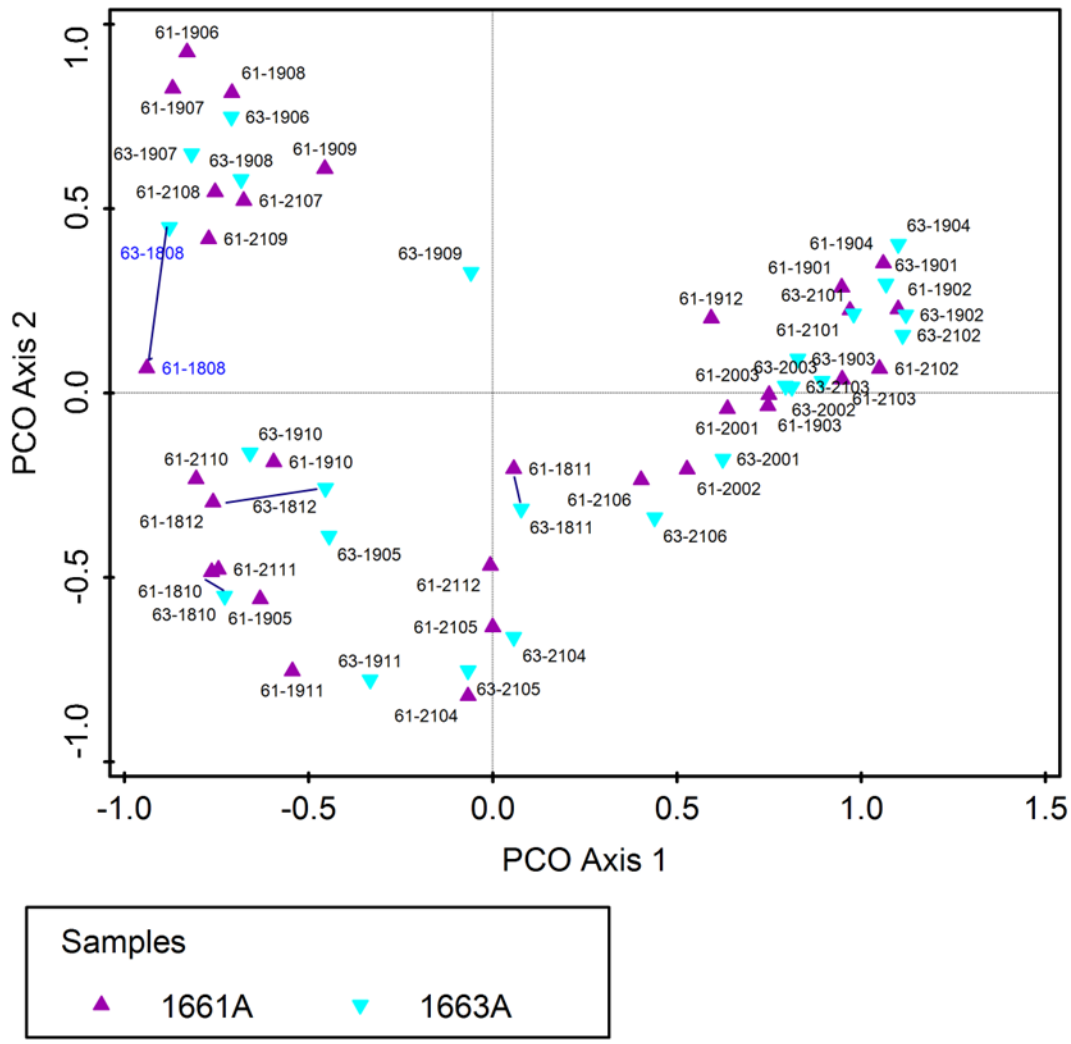

Fig. 23. Comparison of DNA-based phytoplankton at sites 1661A and 1663A from 2018-2021. Each dot represents one sample and is labelled as SITE-YYMM. Samples with blue labels were collected before the closure of OCNGS.

Phytoplankton Changes in Relation to Environmental Variables

CCA analyses were performed to investigate the relations of phytoplankton changes to environmental conditions before and after the OCNGS closure at BB07a (Fig. 24), as well as BB01 and BB09 for comparison (Fig. 25). The before-closure dataset includes monthly/biweekly measurements from April 2014 to August 2018, and the after-closure dataset includes the measurements from September 2018 to December 2021. Water quality parameters containing a complete set of measurements were included for the analyses. The water quality data set is paired with phytoplankton data sampled at the same location and time.

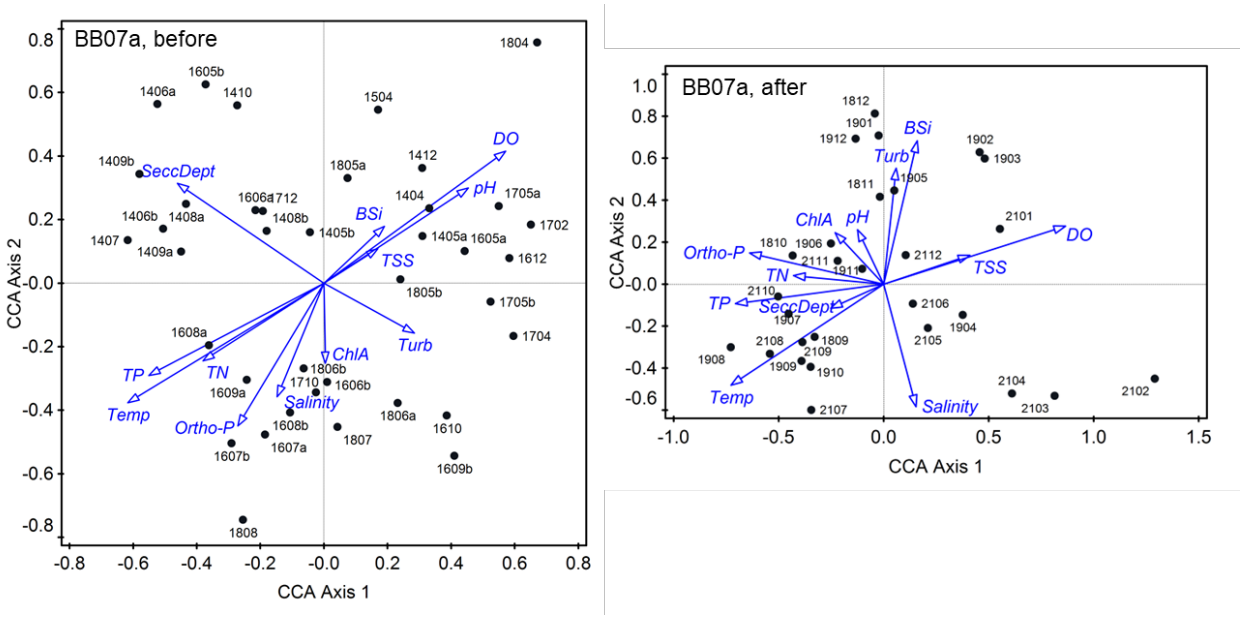

Fig. 24. Changes of phytoplankton in relation to environmental variables derived from CCA at BB07a, before and after the closure of OCNGS. The 'before' dataset includes monthly data from April 2014 to August 2018; the 'after' dataset includes monthly data from September 2018 to December 2021.

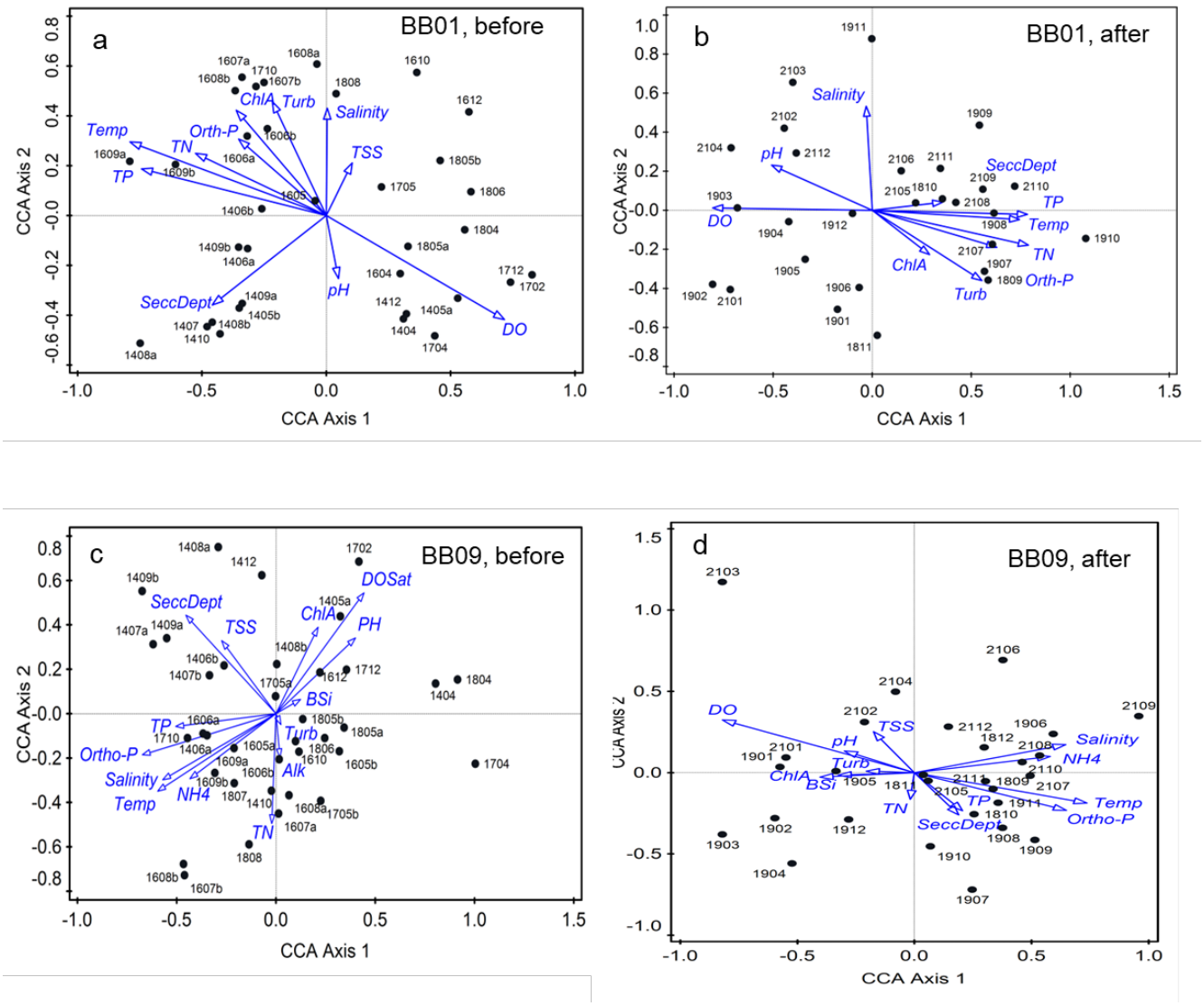

Fig. 25. Changes of phytoplankton in relation to environmental variables derived from CCA at BB01 and BB09, before and after the closure of OCNGS. The 'before' dataset includes monthly data from April 2014 to August 2018; the 'after' dataset includes monthly data from September 2018 to December 2021.

The results from CCA analysis showed that the environmental variables explained 38% of variations in phytoplankton at BB07a before the closure with temperature as the most influential factor, followed by Sechi depth, DO and TP ($p<=0.01$). After the closure, the total effects of environmental variables accounted for 49.8% of the phytoplankton variations, and DO, temperature, and salinity were the most controlling parameters ($p<0.01$) (Fig. 24, Table 4).

The same strategy of CCA analysis was applied to BB01 and BB09, to compare with BB07a. Environmental variables explained 41.7% and 46%, respectively, of phytoplankton composition and abundances changes at BB01 before and after the closure. Before the closure, the most determining variable was temperature, same as BB07a, followed by Secchi depth, salinity, pH, and TP ($p<=0.01$) (Fig. 25a). After the closure, TN became the leading factor explaining phytoplankton variation, different from BB07a, followed by salinity and DO (Fig. 25b). At BB09, the environmental variables accounted for 44.5% and 53.5% of phytoplankton variations 'before' and 'after' OCNGS closure, respectively. Ortho-P and Secchi depth were the leading factors on phytoplankton composition before the closure, which were two controlling factors for BB07a following temperature. After the closure, temperature and DO became the main drivers in phytoplankton changes, which was similar to BB07a (Fig. 25c, 25d, Table 4).

Coincidentally, for all the three sites the explanatory power of the environmental variables increased after the OCNGS closure compared to that before the closure. The difference at BB07a was about 12%, the largest of all three, followed by BB09, about 9%, and BB01 had the least, a little over 4% with the degree of change inversely related to distance from OCNGS (Table 4).

Table 4: Explanatory power of environmental variables on the changes of phytoplankton at BB07a, BB01, and BB09, before and after the closure of OCNGS, derived from CCA analysis. Environmental variables with high significance level are listed.

BB07a	# explanatory variables :	12						
Before decommission					After decommission			
accounted for 38% of community variations					accounted for 50% of community variations			
Name	**Explains %**	**Contribution %**	**pseudo-F**	**P**	**Name**	**Explains %**	**Contribution %**	**pseudo-F**	**P**
Temp	6.2	16.5	2.3	0.002	DO	8.7	17.4	2.5	0.002
Secchi depth	4.4	11.7	1.6	0.008	Temp	6.3	12.6	1.8	0.002
DO	4.5	11.9	1.7	0.002	Salinity	5.1	10.2	1.5	0.006
TP	3.8	9.9	1.4	0.014	Secchi depth	3.8	7.7	1.2	0.172

BB01	# explanatory variables :	11						
Before decommission					After decommission			
accounted for 42% of community variations					accounted for 46% of community variations			
Name	**Explains %**	**Contribution %**	**pseudo-F**	**P**	**Name**	**Explains %**	**Contribution %**	**pseudo-F**	**P**
Temp	7	16.8	2.4	0.002	TN	9.6	19.2	2.6	0.002
Secchi depth	5.3	12.7	1.9	0.002	Salinity	5.8	11.7	1.7	0.004
Salinity	4.6	11	1.6	0.004	DO	5.4	10.9	1.6	0.006
pH	4.4	10.5	1.6	0.006	Ortho-P	4.4	8.9	1.3	0.044
TP	3.9	9.3	1.5	0.016	Turbidity	4.2	8.4	1.3	0.1
TN	3.4	8	1.3	0.064					

BB09	# explanatory variables:	14						
Before decommission					After decommission			
accounted for 44% of community variations					accounted for 53% of community variations			
Name	**Explains %**	**Contribution %**	**pseudo-F**	**P**	**Name**	**Explains %**	**Contribution %**	**pseudo-F**	**P**
Ortho-P	5.3	12	1.9	0.002	DO	8.2	15.3	2.3	0.002
Secchi depth	4.3	9.7	1.6	0.01	Temp	4.7	8.9	1.4	0.046
Chl. *a*	4.4	9.8	1.6	0.018	pH	4.5	8.5	1.3	0.108
TP	3.4	7.7	1.3	0.064	Salinity	4.3	8.1	1.3	0.112

Phytoplankton Metabarcoding

Classification of Autotrophs from 16S Chloroplast Sequences

The classification of the autotrophic phytoplankton from 2020-2021 is plotted together with the 2018 and 2019 samples (Fig. 26-27), derived from the BLASTn analysis of the chloroplast sequences against the PhytoREF database. The results show that the analysis was able to further classify the formerly 'green algae' group (Chloropyceae) in RDP 11 results to eight taxonomic groups including Chlorophytes, Cryptophytes, Euglenophytes, Prymnesiophytes, Chrysophytes, Dictyochophytes, Pelagophytes, and Raphidiophytes. Species in all these groups have been observed and recorded from microscopy analysis previously in Barnegat Bay (Olsen and Mahoney. 2001, Ren 2013, 2015, Fantasia et al. 2017).

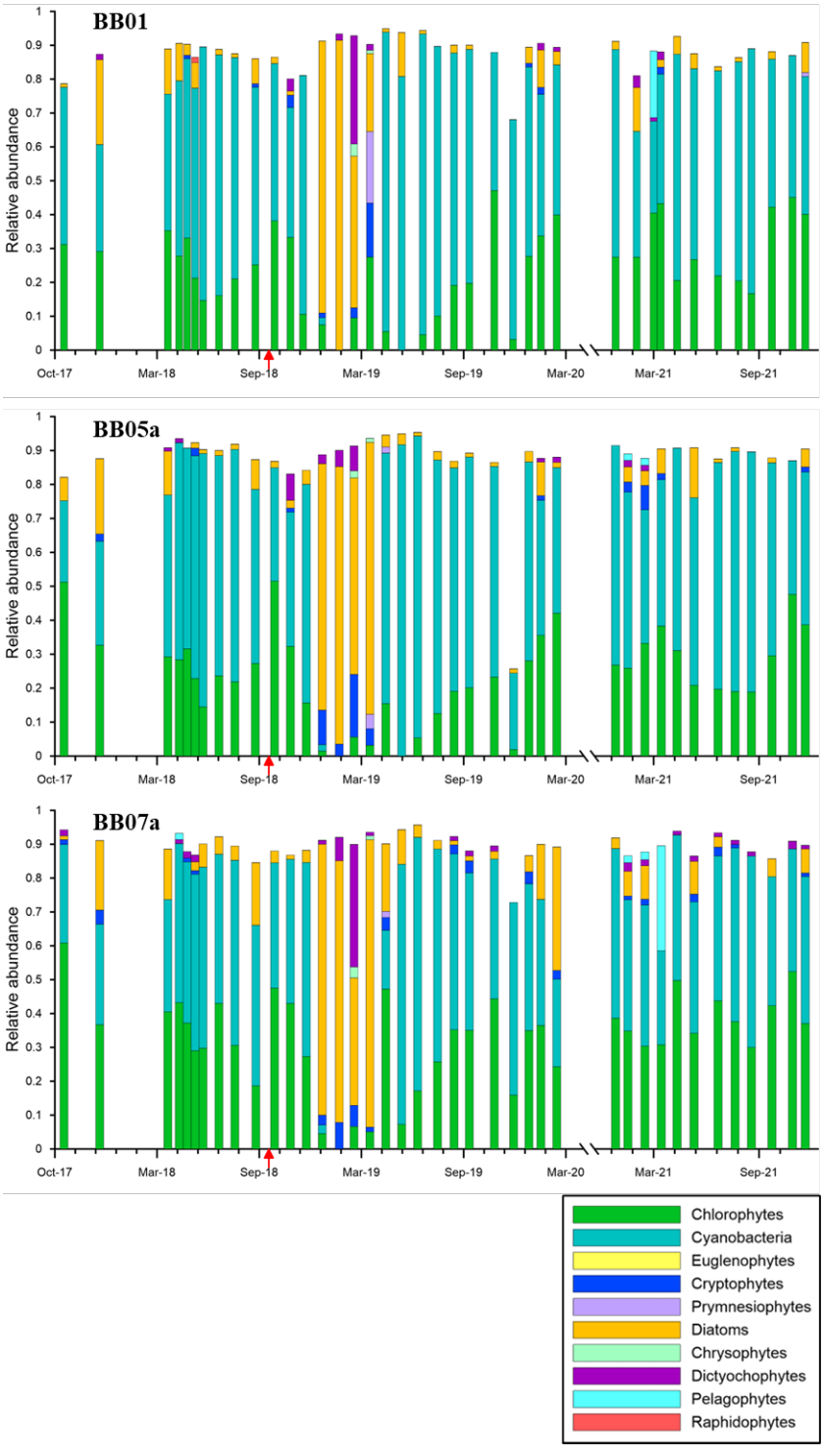

Fig. 26. Composition of phytoplankton classes, based on BLASTn analysis of 16S chloroplast sequences against PhytoREF database, at BB01, BB05a and BB07a. Samples from this three-year study, from 2017/2018 to 2021.

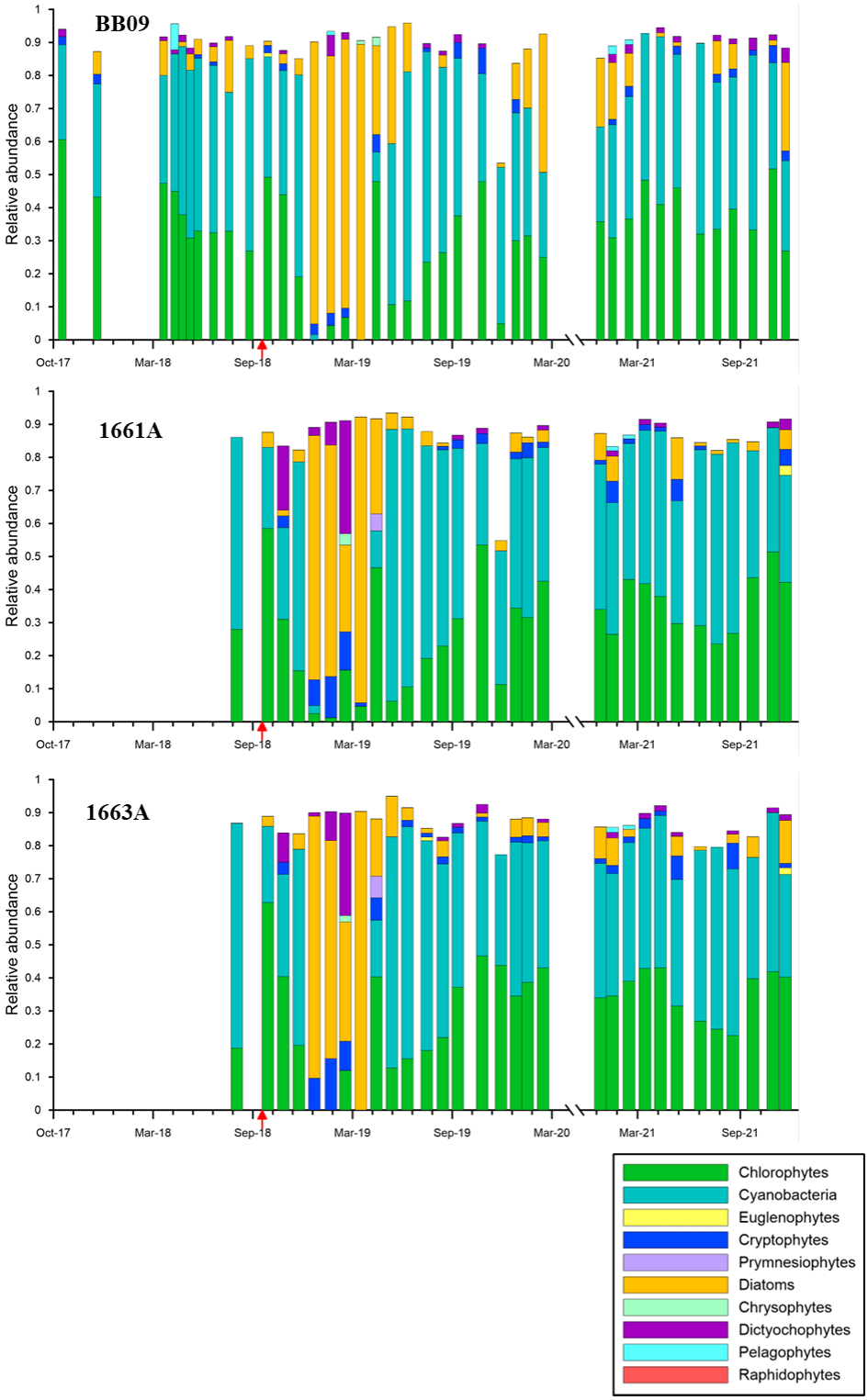

Fig. 27. Composition of phytoplankton classes, based on BLASTn analysis of 16S chloroplast sequences against PhytoREF database, at BB09, 1661A and 1663A. Samples from this three-year study, from 2017/2018 to 2021.

Comparison of Microscopy and 16S Barcoding Results

We used 16S rRNA as gene markers for metabarcoding phytoplankton aiming to include cyanobacteria and eukaryotic algae based on the chloroplast sequences. The comparison of abundant taxa between 16S rRNA-based and microscopy-based classifications was carried out using the 2018 and 2019 samples (Table 5).

The comparison of abundant taxa for the 2018 and 2019 samples is shown in Table 5. The sequences from all the samples were assigned to twelve (12) classes, and most classes were further classified to family level and a few to order. Several species were identified from sequencing data such as diatom *Rhizosolenia setigera*, Prasinophyte *Cymbomonas tetramitiformis*, and Raphidiophyte *Heterosigma akashiwo*, and their occurrence and relative abundance in samples were somewhat in agreement with the microscopic results.

The DNA-based classification revealed several taxonomic groups in the 'picoplankton' complex, including Cyanobacteria *Prochlorococcus* spp. and *Synechococcus* spp., Chlorophyte *Ostreococcus tauri* and some species from family Bathycoccaceae, Eustigmatophyte *Nannochloropsis gaditana*, Prasinophytes *Picochlorum eukaryotum*, *Picocystis salinarum*, and family Pelagomonadaceae (Table 5).

Table 5: Comparison of abundant taxa from 16S metabarcoding and microscopy, updated with 2018& 2019 samples.

Classes	Metabarcoding	Microscopy	Notes
Cyanophyceae	*Prochlorococcus* sp.	Pico-Cyanobacteria	
	Synechococcus sp.	*Synechococcus* sp.	
	Merismopedia tenuissima	*Merismopedia* spp.	Both methods detected the most abundant in the sample of 10/23/2018 from BB05a
Euglenophyceae	*Eutreptiella pomquetensis*	*Eutreptiella* sp.	Main Euglenophytes found in BB-LEH
Cryptophyceae	Chroomonadaceae Pyrenomonadales	*Hemiselmis virescens*	
		Teleaulax acuta	
		Leucocryptos marina	
		Plagioselmis sp.	
		Rhodomonas salina	
Prymnesiophyceae	I*sochrysis* sp.	*Chrysochromulina* sp.	
	Phaeocystaceae		*Prymnesium parvum* detected in marsh ponds in southern Tuckerton Peninsula
	Chromulinaceae		
	Chrysochromulinaceae	*Chrysochromulina* spp.	
	Prymnesiophycidae		
Chrysophyceae	Chromulinaceae	*Paulinella (Calycomonas) ovalis*	
		Calycomonas gracilis	
		Dinobryon belgica	
		Dinobryon faculiferum	
		Pseudopedinella pyriformis	
Raphidophyceae	*Heterosigma akashiwo*	*Heterosigma akashiwo*	
Pelagophyceae	Pelagomonadaceae	*Aureococcus anophagefferens*	
Eustigmatophyceae	Monodopsidaceae		
	Nannochloropsis gaditana		
Dictyochophyceae	Dictyochophyceae	*Dictyocha fibula*	
		Dictyocha spp.	
Bacillariophyceae	Cymatosiraceae	*Arcocellulus* spp.	
	Melosiraceae	*Cerataulina pelagica*	
		Dactyliosolen fragilissimus	
	Skeletonemataceae	*Skeletonema costatum*	
		Skeletonema menzelli	
	Stephanodiscaceae		
	Thalassiosiraceae	*Thalassiosira tenera*	
		Th. (*Minidiscus*) *proschkinae*	
		Thalassiosira weissflogii	
		Thalassiosira nordenskioeldii	
	Thalassiosira pseudonana		
	Rhizosolenia setigera	*Rhizosolenia setigera*	
	Chaetocerotaceae	*Chaetoceros throndsenii* var. t*hrondsenia*	The species was dominant in May-June
		Chaetoceros subtilis	
		Chaetoceros subtilis var. *abnormis* fo. *simplex*	
Prasinophyceae	*Cymbomonas tetramitiformis*	*Cymbomonas tetramitiformis*	Both methods detected the species in samples BB06 on 12/19/2016, and BB05a & BB07a on 6/5/2018
	Pyramimonadaceae	*Pyramimonas plurioculata*	
		Pyramimonas parkeae	
		Tetraselmis spp.	
		Pseudoscourfieldia marina	
		Resultomonas moestrupii	
	Picochlorum eukaryotum	Pico-coccoids	
	Chlorellaceae	Pico-coccoids	

Table 5 (continued): Comparison of abundant taxa from 16S metabarcoding and microscopy, updated with 2018& 2019 samples.

Classes	Metabarcoding	Microscopy	Notes
Chlorophyceae	*Ostreococcus tauri*	Pico-coccoids	
	Mamiellaceae	*Mamiella gilva*	
		Tasmanites marshalliae	
		Micromonas pusilla	
Dinophyceae		*Heterocapsa rotundatum*	
		Kryptoperidinium triquetra	
		Prorocentrum minimum	
		Gyrodinium estuariale	
		Undifferentiated *Gymnodinium* sp. (<20 µm)	

Diatoms are another major component of phytoplankton in Barnegat Bay. About 48 species of diatoms were recorded from 2018 and 2019 samples. Most diatoms are in nano sizes with morphological features that can be distinguished under microscopes with high magnifications. Our study showed that microscopic identification of diatoms was better than 16S metabarcoding, as the former identified most of diatoms to genera and species while the latter assigned only to classes (Table 5). Nevertheless, good correlation between the microscopy and DNA barcoding data sets were achieved for some taxonomic groups, such as for families Skeletonemataceae and Cymatosiraceae (Fig. 28). Microscopic observations recorded two common/abundant species in the family of Skeletonemataceae, *Skeletonema 'costatum'* complex and *S. menzelli*, and two common genera in the family Cymatosiraceae, *Arcocellulus* and *Minutocellus* which includes two species *M. polymorphus* and *M. scriptus*. The correlation between the relative abundance of these families from 16S barcoding and the cell density (in logarithm) from microscopy detection was statistically significant. Furthermore, the comparison revealed the sensitivity of 16S barcoding varied for different taxonomic groups. For Skeletonemataceae and Cymatosiraceae, species with cell counts around 10^4 cells/L in the samples was less likely detected in the barcoding but was detected when their cell density reached above 1.0×10^5 cells/L and their relative abundance was positively correlated to cell counts. For other groups such as *Chaetoceros* species and *Dactyliosolen fragilissimus*, the barcoding was less sensitive, and was able to detect their presence only when the cell counts reached over 1.0×10^6 cells/L (Fig. 29). The comparison also showed that 16S barcoding was sensitive in detecting the presence of some species that were observed occasionally. For example, diatom *Rhizosolenia setigera* made about 3% and 1.8% of relative abundance in the sample collected from BB09 and BB01 on 4/8/2018, respectively. The results are consistent with microscopy data showing the cell counts of 7.5×10^3 and 5×10^3 cells/L, respectively in these samples. Similarly, *Cymbomonas tetramitiformis*, a distinct prasinophycean species, was detected in three same samples by both methods. However, when microscopy detected *Pseudo-nitzschia* spp. at BB07a and BB09 in April 2018, at cell density of 9×10^4 and 1.8×10^5 cells/L, respectively, the 16S barcoding failed to detect the presence of any *Pseudo-nitzschia*. On contrary, the16S metabarcoding detected *Heterosigma akashiwo* in two samples from BB01 and BB07a in June, with relative abundance of 3.2% and 5.9%, respectively, however, microscopy analysis did not catch the species.

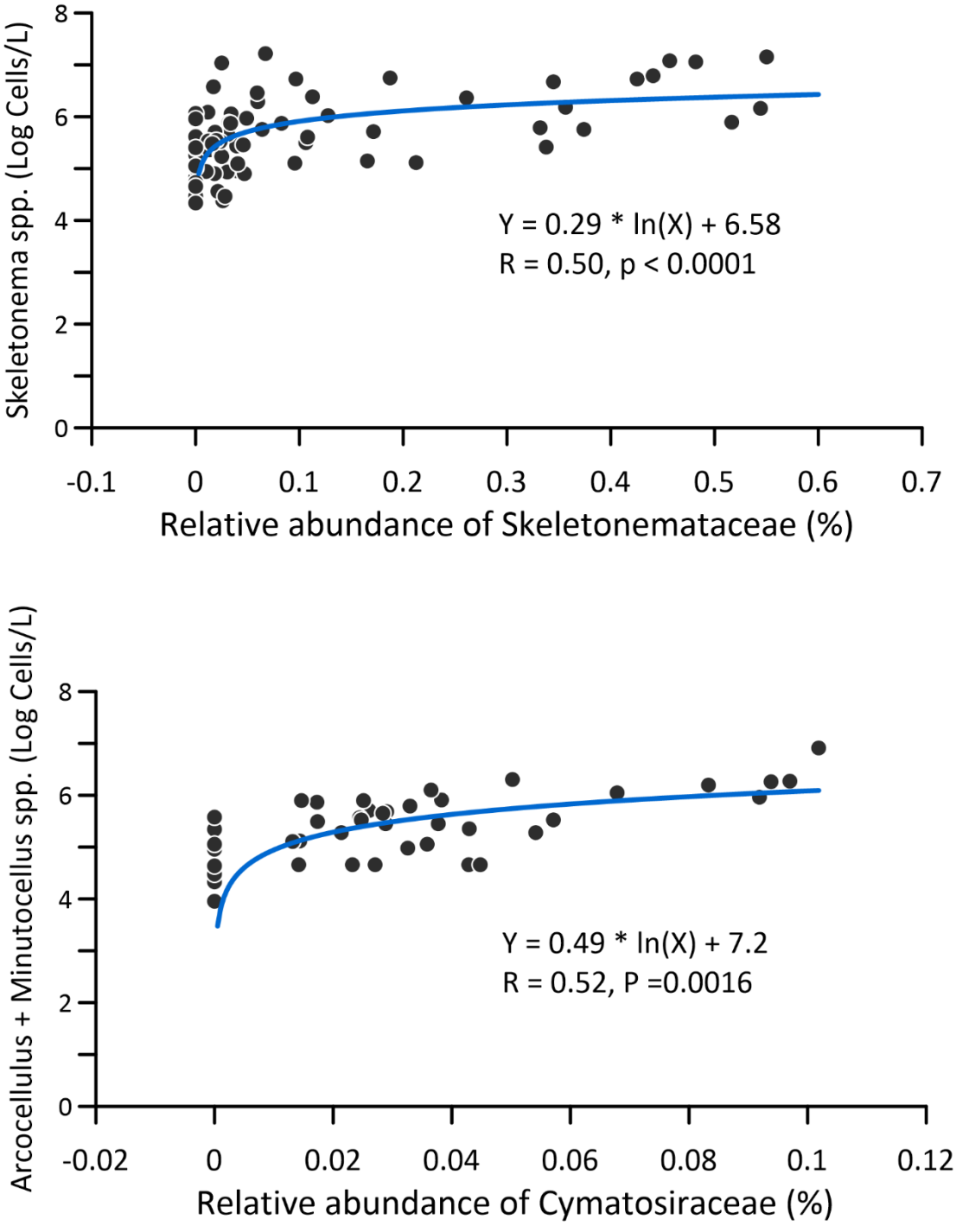

Fig. 28. Comparison of 16S metabarcoding and microscopy datasets on diatoms from 2018 and 2019 samples. Upper: family Skeletonemaceae; Lower: family Cymatosiraceae.

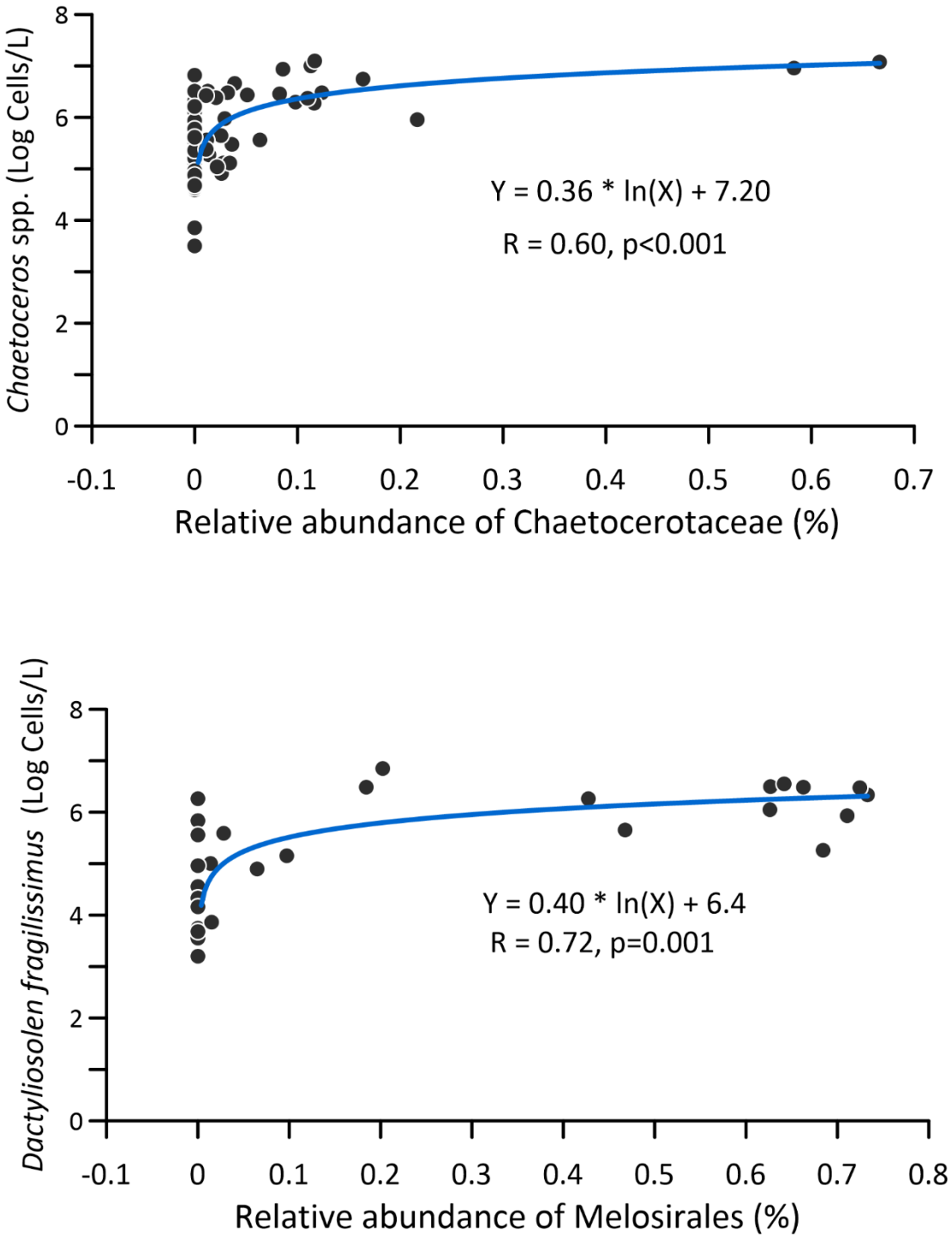

Fig. 29. Comparison of 16S metabarcoding and microscopy datasets on diatoms from 2018 and 2019 samples. Upper: family Chaetocerotaceae; Lower: order Melosirales.

Comparison of three 18S rDNA primers

The tests of the three sets of 18S primers on 24 samples from 2021 showed each primer set has its strength and weakness in classification. 18S-Dino gave better resolution in dinoflagllate classification, as opposed to PhytoD which was the best for diatom classification. 18S-Dino and PhytoD were comparable on the classifications of other major groups. Relatively, V3 87 Oxy primer set was not advantageous in most groups, but it was able to distinguish Prymnesiophytes and the genus *Aureococcus*, which contain *Prymnesium parvum* and brown tide *A. anophagefferens*, respectively, both classified as harmful algae (Table 6).

Table 6: Comparison of three 18S primer sets on the classification of eukaryotic phytoplankton.

	18S-Dino	**V3 87 Oxy**	**PhytoD**	**Remarks**
Phylum (total vs. algae- related)	17 vs. 6	20 vs. 7 (+Rhodophyte)	11 vs. 5 (- Haptophyte)	
Dinoflagellate (genus level)	24	14	8	18S-Dino gives 20 genera, and 4 unclassified
Chlorophyte (genus level)	11	2	7	
Grysta (Diatoms+chryso-+pelago-)	30	14 (no chryso-)	54	
Cryptophytes	5	7	4	
Prymnesiophytes (harmful spp)	+	+	-	
Raphidophytes (harmful spp)	-	-	+	
Aureococcus (harmful AA)	+	+	-	

Discussion

Impact of OCNGS Decommission

Physical and Chemical Changes

The construction and operations of OCNGS altered the hydrology, chemistry and biology of the Forked River, Oyster Creek, and adjacent Barnegat Bay (Summers et al. 1989). Prior to the OCNGS construction, Forked River and Oyster Creek were small, spring-fed, cedar-swamp brooks of typical freshwater and tidal freshwater (salinity ~0.5 ppt) systems (Summers et al. 1989). The construction of the facility changed the flow of the water in Forked River and Oyster Creek and made them a physical extension of Barnegat Bay with salinity ranges around ~25 ppt, similar to that in the center of the Bay (Summers et al. 1989). Sites 1661A and 1663A are located near the mouths of Forked River and Oyster Creek, respectively, and BB07a is southeast of 1663A and closest to OCNGS compared to other BB sites (Fig 1). Salinity changes at these three sites may not be as drastic as inside the Forked River and Oyster Creek, but still there were some evident changes in response to the first step of shutdown around mid-September of 2018. Salinity decreases in the subsequent winter 2018 to early spring 2019 at these three sites suggests a greater influence of freshwater input in the area. This was especially evident at 1661A, which experienced the largest salinity drop among the three sites. The decrease in salinity coincided with the reduction in water intake by the plant from Forked River following the first shutdown steps. In general, salinity in this area of Barnegat Bay is higher in fall-winter and lower in spring-summer owing to the precipitation and associated freshwater discharge in warm seasons. The salinity drop was detected just in fall-winter of 2018. And a slight increase of salinity at 1661A and 1663A was noticeable in the following fall-winter of 2019-2021, consistent with the general trend. In general, both stations exhibited high variability in salinity fluctuations after the OCNGS closure. Although the salinity decrease was short-lived and no permanent trend in salinity decrease was captured through monthly measurements, a shift in relationships between salinity and the other environmental parameters, notably nutrients, was revealed through PCA and CCA analyses, as detailed below.

In previous cases of shutdown at the OCNGS, the sudden temperature drop had reached as much as ~10°C within 15 minutes (e.g. the case of January 2000) and resulted in significant fish mortalities from cold shock (Summers et al. 1989, GPU report 2000). Monthly data from 2018-2021 showed that temperature at 1663A was generally higher than 1661A before the decommission started owing to the discharge of cooling water from OCNGS. However, after the first step of shutdown, the temperature became very similar between these two sites. At BB07a, there was about 4^{o}C of temperature drop in October 2018 compared to other years (Fig. 10). However, a similar decrease of temperature was detected at both BB01 and BB09 in the same month (Fig. 9 and Fig. 11), suggesting more a weather-related (e.g. cold front) change than the

OCNGS closure. The temperature drops and water circulation alteration did not seem abrupt and significant as in previous cases, indicating the effectiveness of a stepwise decommission strategy.

The positive correlations between salinity and nutrients (Ortho-P, ammonia, TN and TP) at BB07a (Fig. 27a) before the shutdown indicate the effects of salt water on the changes of nutrient concentrations. Total freshwater flow into Barnegat Bay from these tributaries typically represents only 2~3% of the tidal prism (Kennish 2001), and most flows into the northern and middle segments of Barnegat Bay, through Toms River and Metedeconk River (Hunchak-Kariouk and Nicholson, 2001). Other tributaries including Forked River and Oyster Creek contribute a much smaller percentage of freshwater input. On the other hand, Barnegat Bay is a shallow and semi-enclosed water body, the changes of nutrients and phytoplankton growth can be very dynamic. A hydrological model demonstrated a pronounced subtidal flow from Barnegat Inlet, transporting marine water into the Southern segment of the Bay (Defne and Ganju 2015). The adjacent Atlantic coast water contains higher concentrations of nutrients, which can be sources for nutrient replenishing especially for the southern segment of the Bay.

The negative relationship between salinity and nutrients after the closure suggests freshwater influences on the changes of nutrients. After the shutdown, with 95% reduction of water circulation through OCNGS, freshwater from the watershed can directly discharge to Forked River and Oyster Creek and further to Barnegat Bay. Though freshwater discharge is not as much as Toms River, the riverine nutrients may have exceeded the input of the oceanic water through Barnegat Inlet.

BB01 is in the northern end of Barnegat Bay and under least impact from the OCNGS. Positive correlation between salinity and nutrients 'before the closure' was similar to BB07a. For the period of 'after the closure,' the weak negative correlation between salinity and TN, suggesting slight influences of freshwater input of nitrogen from Metedeconk River, when TP and ortho-P did not seem to correlate to salinity. The positive correlation between TSS and ortho-P and TP suggests a significant role that sediments play in P distribution and regeneration through particulate phosphorus (PP) in shallow waters, consistent with previous studies (Joshi et al. 2015, Paudel et al. 2017).

BB09 is away from the OCNGS and close to Barnegat Inlet, thus under stronger influences of water exchanges and circulations through the inlet (Defne and Ganju 2015). Same as BB07a, positive correlations between nutrients and salinity suggest some prominent influences of oceanic water in regulating the nutrients in the area before the shutdown. The correlations between salinity and nutrients at BB09 were highly positive before the closure but reversely related afterward, especially TN and TP, which is comparable to BB07a. The bioavailable inorganic nutrients, ortho-P and NH4, showed no correlation with salinity after the closure.

Different from BB07a and BB01, chlorophyll *a* at BB09 seems de-coupled from the variations of nutrients both 'before-' and 'after-' the closure, indicated by their negative correlations.

Phytoplankton Community Changes

Phytoplankton growth and composition can change quickly in response to hydrological, physical, and chemical modification due to their nature of floating, minute sizes and fast-growing rate (O'Boyle and Silke 2010). High dynamics of monthly and inter-annual phytoplankton changes are evident from both DNA and microscopy data in this study period, as well as microscopy data in previous years. Seasonality was prominent every year at each site, driven primarily by temperature. The taxonomic groups/species and diversity of phytoplankton were, in general, comparable from year to year (Ren 2015, 2017).

Our study showed that the changes in phytoplankton community are significantly affected by environmental variables, and phytoplankton growth is significantly affected by nutrients as indicated by the positive correlations between nutrients and ChlA. The environmental variables, led by temperature, salinity, Secchi depth (or turbidity), and nutrients, explained 38% to >53% of phytoplankton changes in Barnegat Bay, this varied between sites. The differences between the 'before-' and 'after-' closure in terms of the relationships of environmental variables with phytoplankton changes and the increased explanatory power can be indications of the impact of OCNGS closure. However, the environmental variables and man-made activities could be intertwined in affecting the phytoplankton changes at short-term and local scales. In particular, temperature can play significant roles in temporal variations of phytoplankton community structure (species composition and abundances), especially in spring and fall, as this study showed, which makes it challenging to compare before- and after-closure communities.

Larger dissimilarity of phytoplankton between the mouth of Forked River (site 1661A) and that of Oyster Creek (site 1663A) in August 2018 compared to the October samples suggests the effects of the first step shutdown on the short-term (months) variability of phytoplankton. Furthermore, the subsequent higher dissimilarity between these two sites in November than in December coincided with the secondary shutdown of the circulation pumps in November. When the flow was reduced following cessation of pump operations, the difference in water temperature and water circulation between the intake (Forked River) and the outflow (Oyster Creek) was consequently reduced. The impact of the closure is consistent with the changes in salinity at 1661A and 1663A. In 2021, more than two years after the initial shutdown, phytoplankton assemblages between the two sites were closely comparable in most months. The exceptions were for March, April, August, and December, when the same degree of dissimilarity as August 2018 was detected between the two sites. These differences were more likely caused by some localized and short-term variability in physical, hydrological and chemical changes as

chlorophyll a, nutrients and TSS and other parameters were noticeably different between the two sites.

The impact of OCNGS decommission may also be evident at BB07a by comparing the samples from the same month from 2012 to 2021, when the effects of temperature were minimized. The highest variability of the August samples exhibited between the years 2012 vs. 2013, and 2018 vs. 2019. When the large variability between 2012 and 2013 resulted from the impact of Hurricane Sandy, the variability between 2018 and 2019 may have been caused by the shutdown of OCNGS. Since BB07a is located closest to the OCNGS, as compared to other BB sites, the results support why the shutdown may have exerted an influence. The shutdown of the water circulation may have resulted in more inflows of freshwater from Oyster Creek to Barnegat Bay near BB07a, which in turn has affected nutrients. A drop of 4-8 ppts in salinity was observed at 1661a and 1663a after the OCNGS decommission, followed by a slight increase and high variability in salinity in 2019to 2021. However, a reverse relationship between salinity and nutrients at BB07a, particularly ortho-P, after the closure suggests an increase in freshwater sources for nutrients. Consequently, the effects of salinity on phytoplankton became significant after the closure (Table 4).

BB09 is further away from OCNGS than BB07a and considered a reference site as well as BB01. These two sites are assumed to receive little or no effect from the OCNGS closure. Phosphorus was the limiting nutrient for phytoplankton growth before the closure. However, after the closure, temperature became the leading factor and a phosphorus effect was much reduced, the same as BB07a. Because of these similarities in ‘before’ and ‘after’ changes between BB09 and BB07a, one may assume slight influences of the OCNGS shutdown to that segment of the Bay. BB01 is located furthest from the OCNGS. Although before the closure, the same as BB07a, temperature and Secchi depth were the leading factors on phytoplankton, after the closure, TN and salinity became the leading ones, which is very different from BB07a. The change in the temperature-nutrients regime found in the reference sites could also indicate impacts from changes in climate conditions over the project time period, and were not necessarily related to the OCNGS closure. However, climate data was not available for this time and this hypothesis cannot be verified.

It is worth noting that the water quality and phytoplankton data were collected monthly. The change of temperature and water circulation following the shutdown happened in a relatively short time and may not be captured through monthly sampling. All the phytoplankton changes we detected at our study sites could result from both the effects of OCNGS decommission and the natural, very dynamic environmental conditions related to hydrological, chemical, and biological processes in Barnegat Bay. From phytoplankton variations over multiple years at every study site, there were many instances where monthly variability between August and

October samples and interannual variability of August samples from 2012 to 2017 were larger than the differences between sampling events made in August to October. In addition, the impact of weather conditions, such as wind, precipitations, tides and small-scale water advection and circulation are not available and cannot be evaluated throughout the sampling period. Overall, the changes observed in phytoplankton assemblages in the months before and after the OCNGS closure are hard to distinguish from phytoplankton natural changes observed between 2012-2017.

Phytoplankton Metabarcoding

16S rRNA-based metabarcoding provides the classifications for cyanobacteria and eukaryotic phytoplankton, which are derived from the chloroplast sequences. The method identified twelve (12) classes, and most classes were further annotated to family level. All the classes were confirmed by microscopy analysis. Moreover, the 16S sequencing method has the advantage of resolving several taxonomic groups in the 'picoplankton' complex, which is generally challenging for morphology-based microscopy analysis. The microscopic method can differentiate pico-sized cyanobacteria from other picoplankton by using green excitation fluorescence (Ren et al. 2009), but the resolution on other groups, especially picoeukaryotes has not been efficient. The 16S sequences from the 2018 and 2019 samples suggested high biodiversity in summer picophytoplankton in BB-LEH.

Compared to 16S barcoding, microscopy has better resolution in identifying diatoms and other nano-sized phytoplankton. The microscopy was able to identify most of the diatoms to genera and species, whereas 16S barcoding assigned only to classes. The lack of resolution in genus and species-level classifications in 16S barcoding is mainly due to the limited diatom references in the PhytoREF database, which contains only 278 reference barcodes of diatoms (http://phytoref.sb-roscoff.fr/). Nevertheless, a significant correlation of four diatom classes, Skeletonemaceae, Cymatosiraceae, Chaetocerotaceae, and Melosirales, between microscopic counts and DNA-based relative abundance was obtained from the 2018-2019 data. The comparison also provides information about the sensitivity of 16S barcoding for different taxonomic groups.

For the detection of harmful algae, when microscopy was able to detect a relatively low density of *Pseudo-nitzschia* in the samples, 16S sequencing did not. Meanwhile, the 16S metabarcoding detected *Heterosigma akashiwo* at low relative abundance (3.2%-5.9%), while the species escaped from microscopy detection, although the species has been encountered occasionally in previous BB-LEH samples at low density (Ren 2015). Several reasons can affect the sensitivity and accuracy of metabarcoding classifications, as discussed in the studies by Bennke et al. (2018) and Esenkulova et al. (2020). Furthermore, the 16S metabarcoding gave the results that

made 0.1% relative abundance. The sensitivity level for individual taxa could be dependent on the community composition and dominant/abundant species (Giner et al. 2016).

It is worth noting that the 16S barcoding may have the tendency to mis-present *Chattonella subsalsa* as *H. akashiwo* (Esenkulova et al. 2020). Regardless, both species are raphidophytes and are associated with fish and shellfish kills (Moestrup et al. 2008, Haigh and Esenkulova 2014).

The main limitation of the 16S barcoding is its lack of detection ability for dinoflagellates. The same issue exists in similar studies (Bennke et al. 2018). The lack of detection of dinoflagellates in the current dataset can be attributed to the underrepresentation of dinoflagellates reference barcodes in the PhytoREF database (0.5% of all entries). The amplification of the 16S rRNA genes of dinoflagellate plastids is much less possible compared to other eukaryotic algae as the genomes of dinoflagellate plastids have usually been broken up, and many genes, including 16S rRNA and 23S rRNA, have been transferred into the nucleus of dinoflagellates (Green 2011).

Our tests showed that 18S rRNA gene amplification can be better used in the resolution of dinoflagellates, especially the 18S-dino that specifically targets dinoflagellates (Esenkulova et al. 2020). The development of new primers targeting dinoflagellate chloroplasts (specifically toxic species) would considerably advance the performance of molecular-based analyses.

Summary

Temporal and spatial variations of phytoplankton at six sites were investigated from 2018-2021 using traditional microscopy and DNA sequencing methods under the Barnegat Bay Phase II program (NJDEP-Barnegat Bay). The monthly and inter-annual changes of phytoplankton at the sites near the mouths of Forked River (1661A) and Oyster Creek (1663A), as well as the long-term monitoring sites BB07a, BB01 and BB09 were analyzed to understand the effects of the OCNGS decommission at the short-term and long-term scale. Water quality data from the same sites and the same time periods as phytoplankton investigations was compiled, retrieving from EPA's Water Quality Portal (https://www.epa.gov/waterdata/water-quality-data-download). The correlations between environmental variables and the relationships between phytoplankton changes and environmental variables were examined from three long-term monitoring sites with a focus on 'before' and 'after' OCNGS closure.

The study showed high dynamics of temporal variations of phytoplankton at each site, significantly affected by environmental variables. Multivariate analyses based on long-term data showed that environmental variables explained about 38% to over 53% of phytoplankton changes from BB01, BB07a, and BB09. Coincidentally, there was an increase in the explanatory power of the environmental variables for all three sites after the OCNGS closure, but with BB07a increasing the most and BB01 the least, coincident with their distances from the OCNGS.

It is also worth mentioning that BB01 is located in an area of Barnegat Bay characterized by lowest salinities and poorest oceanic hydrological influence, which may explain the lowest variability recorded there. As the effects of the environmental variables and man-made activities can often be intertwined, the differences observed at these sampling stations are difficult to disentangle from OCNGS decommission effects.

Meanwhile, the impact of the OCNGS closure may be evident from the following findings:

- The larger dissimilarity of phytoplankton between the mouth of Forked River (site 1661A) and that of Oyster Creek (site 1663A) in August 2018 compared to the October samples coincided with the first step shutdown of OCNGS. Furthermore, the subsequent dissimilarity in November samples between these two sites and more similarity in December samples coincided with the shutdown of the secondary circulation pumps in November. High variations in the following months/years were observed in the similarity/dissimilarity of these two stations.
- A comparison of the phytoplankton at BB07a was made based on the samples collected in August from 2012 to 2021 when the effects of temperature were minimized. The variability of the August samples between 2018 vs. 2019 was comparable to that between 2012 vs. 2013 when the latter was heavily impacted by Hurricane Sandy. For the September samples, the largest dissimilarity was detected from 2018 vs. 2019. The October samples also showed higher distance from 2018 vs. 2019 among the years from 2014-2021. However, similar or larger dissimilarities were occasionally observed for other months during the entire sampling period for phytoplankton assemblages.
- Salinity drops at sites BB07a, 1661A and 1663A were evident in response to the steps of the shutdown, suggesting an increased influence of freshwater in the area. Moreover, a positive relationship between salinity and nutrients was observed at BB07a, BB01 and BB09 before the shutdown. After the shutdown, nutrients showed a reverse relationship to salinity at BB07a and BB09, whereas at BB01which is furthest from the OCNGS, nutrients showed no or weak relation to salinity. Although the Barnegat Bay near the mouths of Forked River and Oyster Creek did not become freshwater dominant as we originally hypothesized, the shutdown of the water circulations from OCNGS have resulted in more direct freshwater inflows from Oyster Creek, which in turn enriched nutrients in the area near BB07a, and possibly BB09. Second, these sites exhibited a shift in the salinity-nutrient relationship before and after the closure, though not as strong as BB07a.
- Phytoplankton metabarcoding was developed using 16S rRNA and 18S rDNA gene markers combined with the microscopy method. The combination of 16S rRNA marker and NextGen Sequencing generated high-throughput data and provided information on

photosynthetic cyanobacteria and eukaryotic phytoplankton, its community diversity and composition, as well as the relative abundance of major taxonomic groups. Significant correlation of four diatom classes, Skeletonemaceae, Cymatosiraceae, Chaetocerotaceae, and Melosirales, between microscopic counts and DNA-based relative abundance was obtained from the 2018-2019 data. Although limitation exists in classification resolution for nano-phytoplankton and dinoflagellates, the method has advantages over light microscopy on picoplankton and was able to distinguish major groups in picoplankton complex, which are often challenging by the traditional microscopy methods. Our study provided a foundation for further research in developing metabarcoding and identified some existing gaps in sequence databases.

- The test of the three sets of 18S rDNA primer sets showed each primer set has its strengths and weaknesses in phytoplankton classification. 18S-Dino gave better resolution in dinoflagellates but was comparable to PhytoREF in terms of the classifications of other phytoplankton groups. The V3 87 Oxy primer set did not appear to be advantageous in most taxonomic groups; however, it was able to distinguish Prymnesiophytes and the genus *Aureococcus*, which contain *Prymnesium parvum* and brown tide *A. anophagefferens*, respectively, both classified as harmful algae.

References

Abad, D., A. Albaina, M. Aguirre, A. Laza-Martínez, I. Uriarte, A. Iriarte, F. Villate, and A. Estonba. 2016. Is metabarcoding suitable for estuarine plankton monitoring? A comparative study with microscopy. Mar Biol 163: 149. doi:10.1007/s00227-016-2920-0

Bennke C.M., F. Pollehne, A. Müller, R. Hansen, B. Kreikemeyer, M. Labrenz. 2018. The distribution of phytoplankton in the Baltic Sea assessed by a prokaryotic 16S rRNA gene primer system, Journal of Plankton Research, 40(3): 244–254, https://doi.org/10.1093/plankt/fby008.

Bush A., Z.G. Compson, M.A. Monk, T.M. Porter, R. Steeves, E. Emilson, N. Gagne, M. Hajibabaei, M. Roy and D.J. Baird. 2019. Studying Ecosystems with DNA Metabarcoding: Lessons From Biomonitoring of Aquatic Macroinvertebrates. Frontiers in Ecology and Evolution. 7:434. doi: 10.3389/fevo.2019.00434

Cole J.R., Q. Wang, J.A. Fish, B. Chai, et al. 2013. Ribosomal Database Project: Data and tools for high throughput rRNA analysis. Nucleic Acids Research. 42: D633-642.

Curry K. D., Q. Wang, M. G. Nute, and others. 2021. Emu: Species-Level Microbial Community Profiling for Full-Length Nanopore 16S Reads.doi:10.1101/2021.05.02.442339

Decelle J., S. Romac, R.F. Stern, E.M. Bendif, A. Zingone, et al. (2015), PhytoREF: a reference database of the plastidial 16S rRNA gene of photosynthetic eukaryotes with curated taxonomy. Mol Ecol Resour, 15: 1435–1445. doi:10.1111/1755-0998.12401

Defne, Z. and N.K. Ganju. 2014. Quantifying the residence time and flushing characteristics of a shallow, back-barrier estuary: Application of hydrodynamic and particle tracking models. Estuaries and Coasts, 38(5), 1719–1734. doi: 10.1007/s12237-014-9885-3

Dortch, Q., R. Robichaux, S. Pool, D. Milsted, G. Mire, N.N. Rabalais, T.M. Soniat, G.A. Fryxell, R.E. Turner and M.L. Parsons. 1997. Abundance and vertical flux of Pseudo-nitzchia in the northern Gulf of Mexico. Marine Ecology Progress Series 146: 249-264.

Esenkulova, S., A. Tabata, B.J.G. Sutherland, N. Haigh. 2020. Combining metabarcoding and morphological approaches to identify phytoplankton taxa associated with harmful algal blooms. doi: https://doi.org/10.1101/816926

Fantasia, R.L., V. M. Bricelj, and L. Ren, 2017. Phytoplankton community structure based on photopigment markers in a mid-Atlantic U.S. coastal lagoon: significance for hard clam production. Journal of Coastal Research, SI 78: 106-126.

Gillevet, P., M. Sikaroodi, et al. 2010. Quantitative assessment of the human gut microbiome using multitag pyrosequencing. Chem Biodivers 7(5): 1065-1075.

Giner, C. R., I. Forn, S. Romac, R. Logares, C. de Vargas, and R. Massana. 2016. Environmental Sequencing Provides Reasonable Estimates of the Relative Abundance of Specific Picoeukaryotes. Appl Environ Microbiol 82: 4757–4766. doi:10.1128/AEM.00560-16

GPU Fish kill monitoring for January 2000. Submitted to NJDEP in 2000, by GPU Nuclear Inc.

Green, B. R. 2011. Chloroplast genomes of photosynthetic eukaryotes. The Plant Journal 66: 34–44. doi:10.1111/j.1365-313X.2011.04541.x

Guillou, L., D. Bachar, S. Audic, and others. 2012. The Protist Ribosomal Reference database (PR2): a catalog of unicellular eukaryote Small Sub-Unit rRNA sequences with curated taxonomy. Nucleic Acids Research 41: D597–D604. doi:10.1093/nar/gks1160

Haigh N, and Esenkulova S. 2014. Economic losses to the British Columbia salmon aquaculture industry due to harmful algal blooms, 2009–2012. PICES Scientific Report No. 47. pp. 2–6.

Hugerth, L. W., E.E.L. Muller, Y.O.O. Hu, L.A.M. Lebrun, H. Roume, D. Lundin, P. Wilmes, and A. F. Andersson. 2014. Systematic Design of 18S rRNA Gene Primers for Determining Eukaryotic Diversity in Microbial Consortia C.R. Voolstra [ed.]. PLoS ONE 9: e95567. doi:10.1371/journal.pone.0095567.

Hunchak-Kariouk, K. and R. S. Nicholson. 2001. Watershed contributions of nutrients and other nonpoint source contaminants to the Barnegat Bay-Little Egg Harbor estuary. Journal of Coastal Research 32:28-81.

Joshi, S., R. Kukkadapu, D. Burdige, M. Bowden, D. Sparks, and D. Jaisi. 2015. Organic Matter Remineralization Predominates Phosphorus Cycling in the Mid-Bay Sediments in the Chesapeake Bay. Environmental science & technology 49. doi:10.1021/es5059617

Kennish, M.J. 2001. Physical description of the Barnegat Bay–Little Egg Harbor estuarine system. In: Kenish, M.J. (ed.), Characterization of the Barnegat Bay – Little Egg Harbor, New Jersey, Estuarine aystem and watershed assessment. Journal of Coastal Research, Special Issue No. 32, pp. 13–27.

Kerkhof, L.J., K.P. Dillon, M.M. Häggblom, and L.R. McGuinness. 2017. Profiling bacterial communities by MinION sequencing of ribosomal operons. Microbiome 5: 116. doi:10.1186/s40168-017-0336-9

Moestrup, Ø., Codd, G.A., Elbrächter, M., Faust, M.A., Fraga, S., Fukuyo, Y., et al. 2008. IOC-UNESCO taxonomic reference list of harmful micro algae [online]: Available from marinespecies.org/HAB.

O'Boyle, S., and J. Silke. 2010. A review of phytoplankton ecology in estuarine and coastal waters around Ireland. Journal of Plankton Research 32: 99–118. doi:10.1093/plankt/fbp097.

Olsen, P., and J.B. Mahoney. 2001. Phytoplankton in the Barnegat Bay-Little Egg Harbor system: species composition and picoplankton bloom development. J. Coast. Res. Special Issue No. 32: 115-143.

Paudel, B., N. Weston, J. Connor, L. Sutter, and D. Velinsky. 2017. Phosphorus Dynamics in the Water Column and Sediments of Barnegat Bay, New Jersey. Journal of Coastal Research 78: 60–69. doi:10.2112/SI78-006.1

Ren, L., N.N.Rabalais,; Turner, R.E.; Morrison, W., and Mendenhall, W., 2009. Nutrient limitation on phytoplankton growth in Upper Barataria Basin, Louisiana: Microcosm bioassays. Estuaries and Coasts, 32, 958–974.

Ren, L. 2013. Baseline Characteristics of phytoplankton and harmful algal blooms in Barnegat Bay-Little Egg Harbor estuary (Year-One). The Academy of Natural Sciences of Drexel University. Technical report to New Jersey Sea Grant and New Jersey DEP.

Ren, L. 2015. Baseline characteristics of phytoplankton and harmful algal blooms in Barnegat Bay-Little Egg Harbor estuary (Year-Two). The Academy of Natural Sciences of Drexel University. Technical report to New Jersey Sea Grant and New Jersey DEP. http://nj.gov/dep/dsr/barnegat/final-reports/phytoplankton-year2.pdf.

Ren, L., T. J. Belton, R. Schuster, and M. Enache. 2017. Phytoplankton Index of Biotic Integrity and Reference Communities for Barnegat Bay–Little Egg Harbor, New Jersey: A Pilot Study. Journal of Coastal Research 78: 89–105. doi:10.2112/SI78-009.1

Ruppert, K. M., R.J. Kline, and M.S. Rahman. 2019. Past, present, and future perspectives of environmental DNA (eDNA) metabarcoding: A systematic review in methods, monitoring, and applications of global eDNA. Global Ecology and Conservation 17: e00547. doi:10.1016/j.gecco.2019.e00547

Santoferrara, L. F. 2019. Current practice in plankton metabarcoding: optimization and error management. Journal of Plankton Research 41: 571–582. doi:10.1093/plankt/fbz041

Summers, J.K., A.F. Holland, S.B. Weisberg, L.C. Wendling, C.F. Stroup, R.L. Dwyer, M.A. Turner, and W. Burton. 1989. Technical review and evaluation of thermal effects studies and cooling water intake structure demonstration of impact for the Oyster Creek Nuclear Generating Station. Revised final report prepared for New Jersey Department of Environmental Protection.

ter Braak C.J.F., and P. Šmilauer. 2012. CANOCO reference manual and CanoDraw for Windows. User's guide: software for canonical community ordination. Version 5.0. Microcomputer Power, Ithaca, NY, USAYoon, et al. 2016. Development of a cost-effective metabarcoding strategy for analysis of the marine phytoplankton community. Peer J 4:e2115; DOI 10.7717/peerj.2115.

Vaulot, D., S. Geisen, F. Mahé, and D. Bass. 2022. pr2-primers: an 18S rRNA primer database for protists. Mol Ecol Resour. 22(1):168-179.

Weigand, H., A.J. Beermann, F. Čiampor, and others. 2019. DNA barcode reference libraries for the monitoring of aquatic biota in Europe: Gap-analysis and recommendations for future work. Science of The Total Environment 678: 499–524. doi:10.1016/j.scitotenv.2019.04.247

Yoon et al. 2016. Development of a cost-effective metabarcoding strategy for analysis of the marine phytoplankton community. Peer J 4:e2115; DOI 10.7717/peerj.2115.

Zhang Z., S. Schwartz, L. Wagner, and W. Miller. 2000. "A greedy algorithm for aligning DNA sequences," J Comput Biol 2000; 7(1-2):203-14.

Zimmermann J.J.R., and J. Gemeinholzer 2011. Barcoding diatoms: evaluation of the V4 subregion on the 18S rRNA gene, including new primers and protocols. Organisms Diversity & Evolution, 11(3): 173 (2011).

Titles of Figures and Tables